Supporting information for:

Design, Synthesis and Characterization of Fibroblast Activation Protein Targeted Pan-Cancer Imaging Agent for Fluorescence-Guided Surgery of Solid Tumors.

Ramesh Mukkamala[1], Spencer D Lindeman[1], Kate A Kragness[1], Imrul Shahriar[1], Madduri Srinivasarao[1] and Philip S. Low[1]*.

Author's Affiliations: [1]Department of Chemistry and Institute for Drug Discovery, Purdue University, West Lafayette, Indiana 47907, United States

Corresponding Author: * Philip S Low, Department of Chemistry, Purdue University, 720 Clinic Dr., West Lafayette IN 47907. Email: plow@purdue.edu, Phone: (765)494-5283, Fax: (765)496-2677

Table of contents:

Experimental Section

Materials and methods:

All anhydrous solvents N,N-dimethylformamide (DMF), tetrahydrofuran(THF), Methanol, dichloromethane (DCM), acetonitrile(ACN) and reagents N,N-Diisopropylethylamine (DIPEA), triethylamine (TEA), Phosphorus oxychloride ($POCl_3$), trifluoroacetic acid (TFA), 1-[Bis(dimethylamino)methylene]-1H-1,2,3-triazolo[4,5-b] pyridinium 3-oxid hexafluorophosphate (HATU), N-Fmoc-ethylenediamine hydrochloride (Fmoc-EDA.HCl), sodium borohydride ($NaBH_4$), and all other chemical reagents were purchased from Sigma-Aldrich. Whereas PEG linkers were purchased from BroadPharm. Cell culture reagents such as Roswell Park Memorial Institute medium 1640 (RPMI 1640), Dulbecco's Modified Eagle's Medium (DMEM) and Eagle's Minimum Essential Medium (EMEM) were purchased from GIBCO, whereas fetal bovine serum (FBS), 1% penicillin-streptomycin, and 2mM glutamine were purchased from Life Technologies. HC Matrigel was purchased from BD Biosciences. All the intermediates and final compounds were purified by either Teledyne combiflash or preparative reverse phase (RP)-HPLC (Waters, xTerra C18 10 µm; 19 × 250 mm) and UHPLC (Acquity, BEH C18, 1.7 µm, 2.1 × 50 mm) as mentioned in experiment section. ^{1} H and ^{13}C NMR spectra were acquired with a Bruker 500 and 125 MHz NMR spectrometer equipped with a TXI cryoprobe. All the proton signals are recorded in ppm with reference to residual $CDCl_3$ (7.26 ppm), CD_3OD (3.34 ppm) and DMSO (2.50 ppm), and data are reported as s = singlet, d = doublet, t = triplet, q = quartet, m = multiplet or unresolved, and b = broad, with coupling constants in Hz. LC/MS analyses were obtained using a Waters micro mass ZQ 4000 mass spectrometer coupled with a UV diode array detector. High resolution mass spectrometric results were obtained by ESI mass using an Applied Biosystems (Framingham, MA) Voyager DE PRO mass spectrometer.

Stable Transduction of HT1080 with hFAP

Six million HT1080 cells were cultured in 100 mm petri dishes with media consisting of DMEM and 10% FBS. The transfection solution was prepared by first mixing 30 µg of Lipofectamine per milliliter of Opti-MEM media. A second solution was prepared by mixing 4 µg FAP expression vector with 10 µg packing plasmid per milliliter of Opti-MEM media, then added to the Lipofectamine solution in drop-wise fashion. The culture media was aspirated from the petri dish, then two milliliters of the resulting solution were added dropwise onto the cells. DMEM media

was added, and the cells were returned to the incubator. After 24 hours, the media was removed and chilled on ice. The media was centrifuged at 500 rcf, then filtered with a 0.45 μm membrane to remove cellular debris. 1 mL of Lenti-X Concentrator was added for every 3 mL of media, and the solution was incubated overnight at 4°C. The virus was concentrated by centrifuging the solution at 1500 rcf and 4°C. The supernatant was discarded, and the virus was redissolved in cold PBS. The virus was diluted with media consisting of EMEM, 10% FBS, and 1% penicillin-streptomycin. The solution was added to a small flask containing 250,000 HT1080 cells. After incubating overnight, the virus-containing media was replaced with complete EMEM and 1 μg of Puromycin per milliliter of media to select for transducted cells. HT1080-FAP cells were cultured and passaged under the same conditions for several weeks. Ten million HT1080-FAP cells were then harvested with Accutase, concentrated in staining buffer, and stained with human FAPα APC-conjugated antibody (R&D Systems) for 20 minutes at 4°C. After washing 3x with staining buffer, dead cells were marked with 7-AAD. The cells were sorted with a BD LSRFortessa Flow Cytometer in the Bindley Bioscience Center to isolate HT1080 cells expressing high quantities of FAP receptor. The high FAP expressing HT1080 cells were cultured and stored for subsequent confocal and binding studies.

Cell culture:

FaDu, HT29, MDA-MB231, KB, 4T1, PANC1, U87MG, and human FAP-transfected HT1080-FAP cells were cultured in a medium consisting of RPMI 1640, DMEM and EMEM, 10% FBS, 1% penicillin-streptomycin, 1% 2 mM glutamine at 37°C in a 5% CO_2 and 95% humidified atmosphere. The cells used in this study was initiated by thawing frozen vials from a master stock saved from the original cell lines purchased from ATCC. All the experiments were performed with in two to five passages following thawing of the cells. No mycoplasma test was performed for any of the cell lines.

In Vitro Enzyme inhibition (IC_{50}) Assays:

FAPα, DPP4, and PREP recombinant enzymes were purchased from R&D Systems. Enzyme buffer was purchased from BPS Bioscience. H-Gly-Pro-AMC and Z-Gly-Pro-AMC were purchased from Bachem Americas, Inc. Briefly, FTL-S-base-ligand (**3)** and FTL-S-S0456) **(4)** concentration (ranging between 10^{-4} and 10^{-11} M) was incubated with enzymes, 1 μM substrate, and buffer in a total volume of 100 μL for 30 minutes at 37°C. Final enzyme concentrations were

50 ng, 25 ng, and 10 ng for FAP, PREP, and DPP4 respectively. The FTL-S-base-ligand **(3**) and FTL-S-S0456 (4) were preincubated with the enzyme for 10 minutes at room temperature before addition of substrate. Fluorescence was measured with a BioTek Synergy Neo2 plate reader in the Chemical Genomics Facility. The excitation wavelength was 365 nm, and the emission wavelength was 450 nm. Conditions were tested in triplicate.

Confocal microscopy:

Human FAP-transfected HT1080-FAP cells were (100,000) were plated on 4 well confocal plates and incubated with various concentration ranging from 100 nM, 50 nM, 25nM and 12.5 nM 6.25 nM concentration of FTL-S-S0456 conjugate (**4)** for 1 h at 37^{o}C. The unbound fluorescence was removed by washing the cells (3x500 µL) with medium, and cell-bound fluorescence was imaged using an Wide-field Nikon microscopy. The experiments were done in triplicates. For colocalization studies 2 µl of Celllight late endosomes-GFP marker (Invitrogen by thermo fisher scientific) was added to HT1080-FAP cells (10,000 cells/well) then incubated at 37 ^{o}C for 16 h, followed by removed the growth media and then incubated with FTL-S-S0456 conjugate (**4**) for 1h at 37 ^{o}C. The unbound fluorescence was removed by washing the cells (3x500 ul) with media and cell-bound fluorescence was imaged using wield-field Nikon microscopy.

In vitro fluorescence binding assay:

100,000 HT1080-hFAP and HT1080 cells were seeded in amine-coated 24 well plates, to ensure cell adherence. Upon formation of a monolayer, cells were incubated with various concentrations of the FTL-S-S0456 dye conjugate (**4**) in the presence or absence of excess of unlabeled FTL-S ligand at 4 ^{o}C. After incubation for 1 h, the cells were washed with (3x 2% FBS in PBS) to remove unbound fluorescence. Finally, cells were dissolved in 300 µl of 1% SDS and 200 µl of cells were transfer into 96 well black plate. The cell-bound fluorescence was measured using a fluorescence spectrophotometer (NeO_2 Plate reader) set with a λex= 745 nm and λ_{em}= 810 nm. Cell-bound fluorescence was plotted against various concentrations and the apparent K_d determined by using one-site binding (hyperbola) curve fit in GraphPad prism7. The experiment was done in triplicates.

Animal husbandry:

5-6 weeks old female athymic nu/nu mice and BALB/c mice were purchased from Harlan Laboratories and Charles River respectively and allowed access to normal rodent chow and water ad libitum. The animals were maintained on a standard 12 h light-dark cycle. All animal procedures were approved by the Purdue Animal Care and Use Committee (PACUC).

In vivo fluorescence imaging and biodistribution:

Female nu/nu athymic (5-6 weeks old) mice were subcutaneously injected with 5 x 10^6 KB, MDA-MB231, HT29, U87MG, FaDu, PANC-1 (cells with 20% matrigel) and 4T1 (in BALB/c mice) cells in 0.1 mL sterile PBS. Tumors were allowed to grow to approximately 400-600 mm^3 before initiating imaging studies, tumor growth was measured perpendicular directions every 2 days using a caliper, and the volumes of the tumors were calculated as $0.5 \times L \times W^2$ (L = longest axis and W = axis perpendicular to L in millimeters). Each tumor-bearing mouse was intravenously injected (via tail vein) with the 5.0 nmol of fluorescent dye conjugate (FTL-S-S0456) either in the presence or absence of a 100-fold excess of unlabeled ligand (FTL-S-base ligand). For whole body imaging and biodistribution studies animals were euthanized 2h post injection by CO_2 asphyxiation. For time course imaging studies animals were imaged under anesthesia using isoflurane at different time points 2h to 120 h). All the whole body and biodistribution images were acquired using Spectral Ami Optical Imaging System. After performing whole-body imaging, organs of interest were harvested and imaged to quantitate fluorescence accumulation using AMI imager. The image acquisition parameters were as follows: i) lamp level-high, ii) excitation-745 nm, iii) emission-810, iv) binning (M) 4M, (v) f-stop-4, (vi) FOV-12.5, (vii) acquisition time, 5 seconds. (viii) power 55. Region of interest (ROI) analysis of tissues were calculated using Aura software. The mean fluorescence (Photons/s/cm^2/sr) from each respective tissues after background subtraction were used for calculation of tumor to healthy tissues ratios (Tumor: heart, tumor: lung, tumor: liver, tumor: spleen, tumor: stomach, tumor: intestine, tumor: kidney and tumor: muscle).

Pharmacokinetic Study: healthy female nude mice were intravenously injected with 10 nmol/mouse of FTL-S-S0456. Blood was collected at regular intervals (5−180 min), and serum

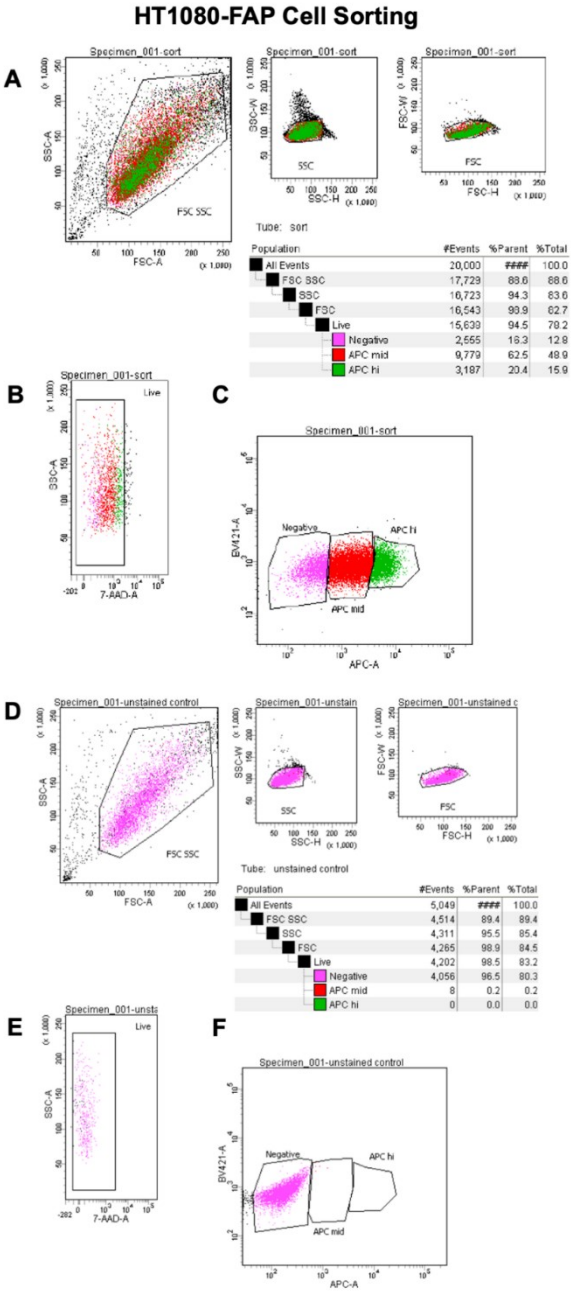

bound FTL-S-S0456 was quantified by measuring the fluorescence using AMI imager. The half-life of FTL-S-S0456 was calculated as % serum bound fluorescence vs time.

Fig. S1 Flow cytometry validation and sorting of HT1080-FAP transduction. HT1080-FAP cells stained with an anti-FAP alpha APC-conjugated antibody were gated by forward and side scatter (A), live cells (B), and high FAP expression (C). An unstained sample of HT1080-FAP cells were gated with a similar strategy (D-E) as a control.

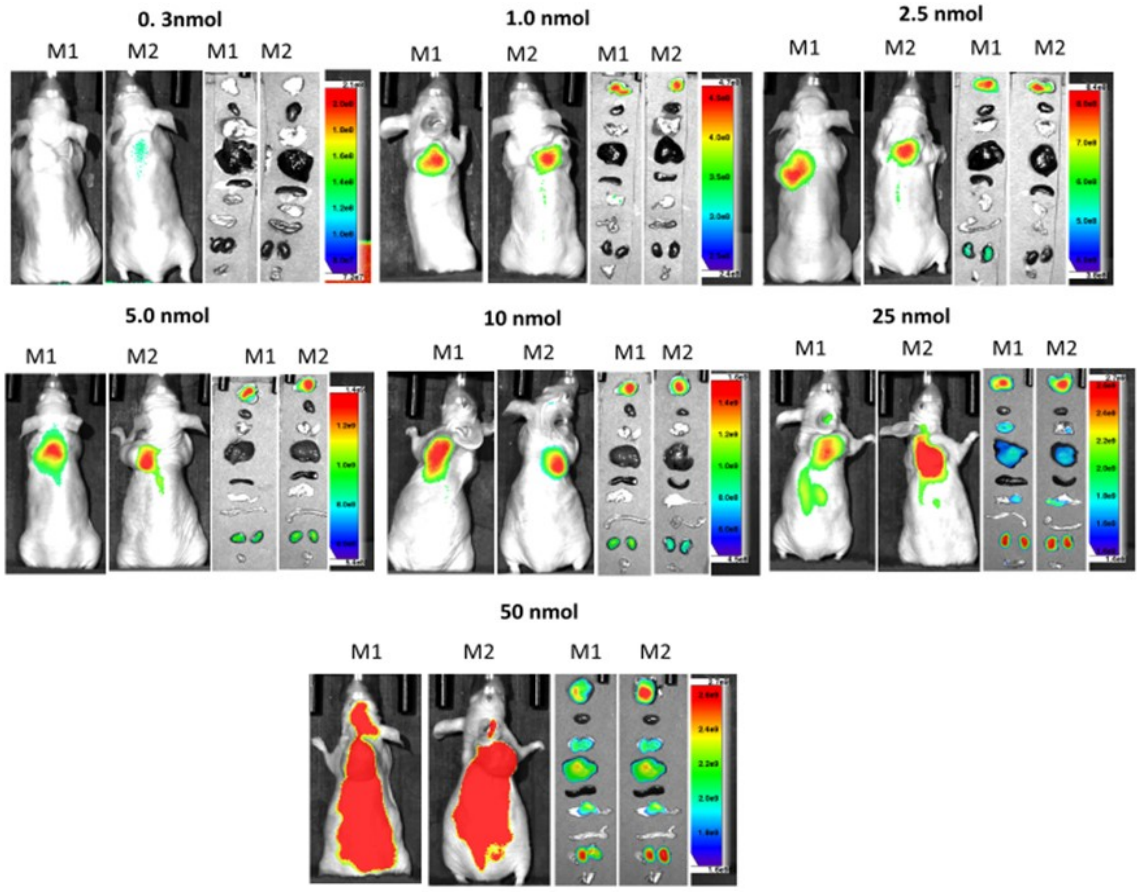

Fig. S2 Determination of the optimal FTL-S-S0456 dose for tumor-specific imaging of KB tumor-bearing mice. Mice were implanted with FAP-negative KB cancer cells and tumors were allowed to grow to ~400 mm^3 in size. Mice were then injected with the indicated nmoles of FTL-S-S0456 and imaged 2h later. After imaging, tissues/organs were dissected and imaged separately. The organs shown from top to bottom are: tumor, heart, lung, liver, spleen stomach, small intestine, kidneys and muscle**.**

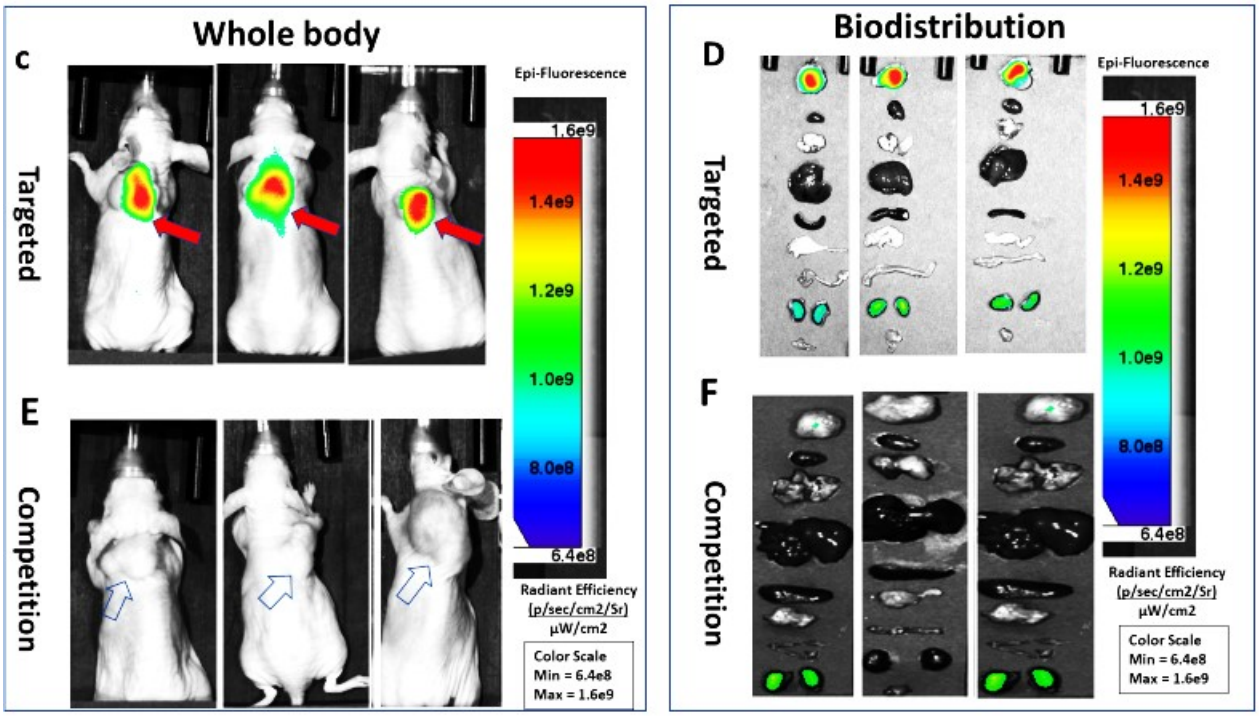

Fig. S3 In Vivo whole-body optical imaging and biodistribution of FTL-S-S0456 in KB tumor bearing mice (n = 5). KB tumor cells ($5x10^6$ cells /mouse) implanted in female athymic nu/nu mice and tumors were allowed to grow to ~400 mm^3 prior to intravenous injection of 5 nmol FTL-S-S0456 (**4**) either in the absence (**A** in whole body and biodistribution images) or presence (**B** whole body and biodistribution images) of excess FAP-ligand **3**. Two hours post injection mice were euthanized and imaged using an AMI imager. Mice from panels **A** and **B** were dissected and the biodistribution of FTL-S-S0456 is shown in the fluorescence images of panels **A** (targeted) and Panel **B** (competition). The tissues examined from top to bottom are tumor, heart, lungs, liver, spleen, stomach, small intestine, kidneys, and muscle.

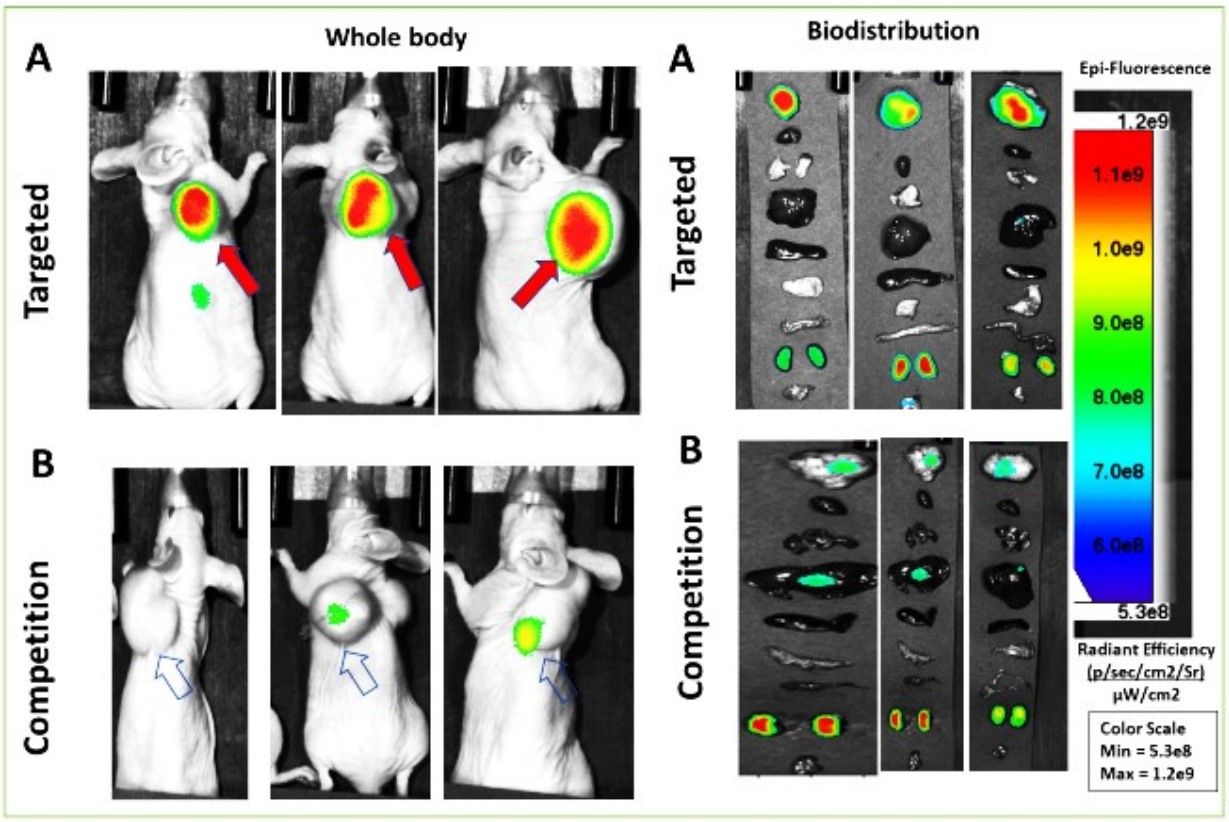

Fig. S4 In Vivo whole-body optical imaging and biodistribution of FTL-S-S0456 in MDA-MB-231 tumor bearing mice (n = 5). MDA-MB-231 tumor cells implanted in female athymic nu/nu mice and tumors were allowed to grow to ~400 mm^3 prior to intravenous injection of 5 nmol FTL-S-S0456 (**4**) either in the absence (**A** in whole body and biodistribution images) or presence (**B** whole body and biodistribution images) of excess FAP-ligand **3**. Two hours post injection mice were euthanized and imaged using an AMI imager. Mice from panels **A** and **B** were dissected and the biodistribution of FTL-S-S0456 is shown in the fluorescence images of panels **A** (targeted) and Panel **B** (competition). The tissues examined from top to bottom are tumor, heart, lungs, liver, spleen, stomach, small intestine, kidneys, and muscle.

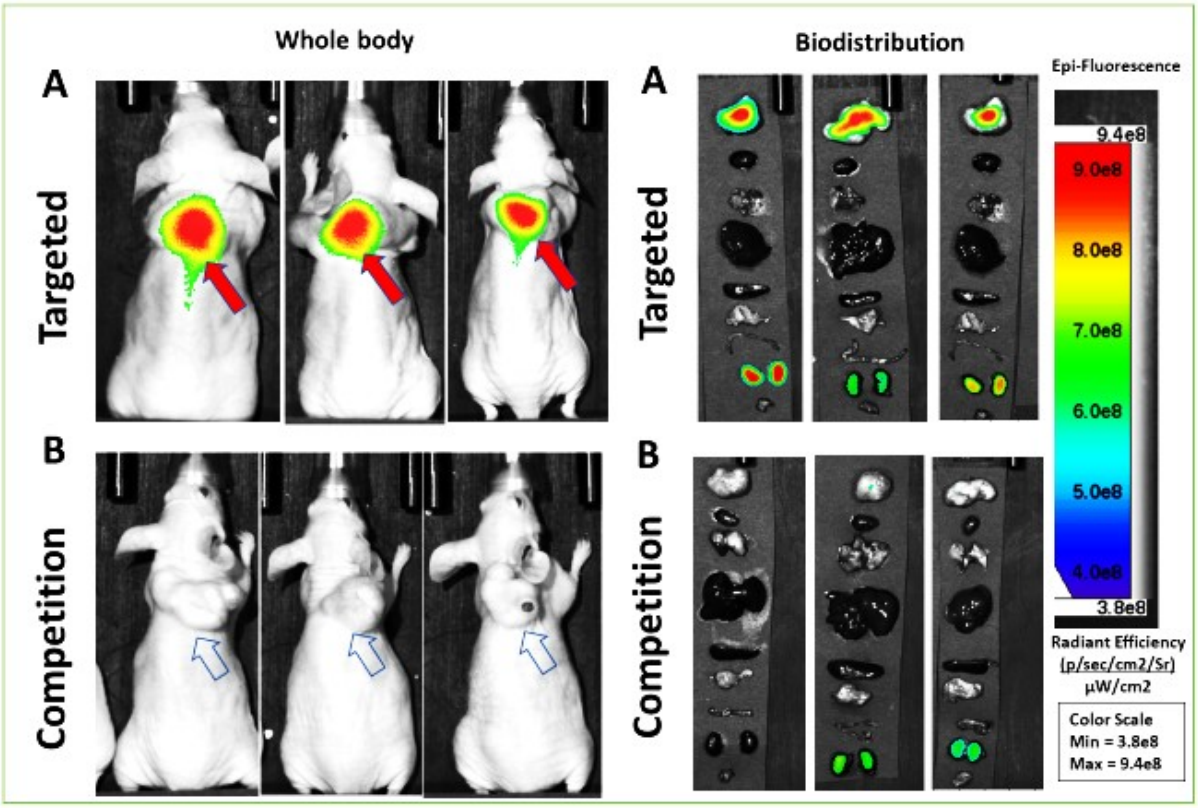

Fig. S5 In Vivo whole-body optical imaging and biodistribution of FTL-S-S0456 in HT29 tumor bearing mice (n = 5). HT29 tumor cells were implanted in female athymic nu/nu mice and tumors were allowed to grow to ~400 mm^3 prior to intravenous injection of 5 nmol FTL-S-S0456 (**4**) either in the absence (**A** both in whole body and biodistribution images) or presence (**B** both in whole body and biodistribution images) of excess FAP-ligand **3**. Two hours post injection mice were euthanized and imaged using an AMI imager. Mice from panels **A** and **B** were dissected and the biodistribution of FTL-S-S0456 is shown in the fluorescence images of panels **A** (targeted) and Panel **B** (competition). The tissues examined from top to bottom are tumor, heart, lungs, liver, spleen, stomach, small intestine, kidneys, and muscle. Red arrow indicates tumor and n =5 mice per/group

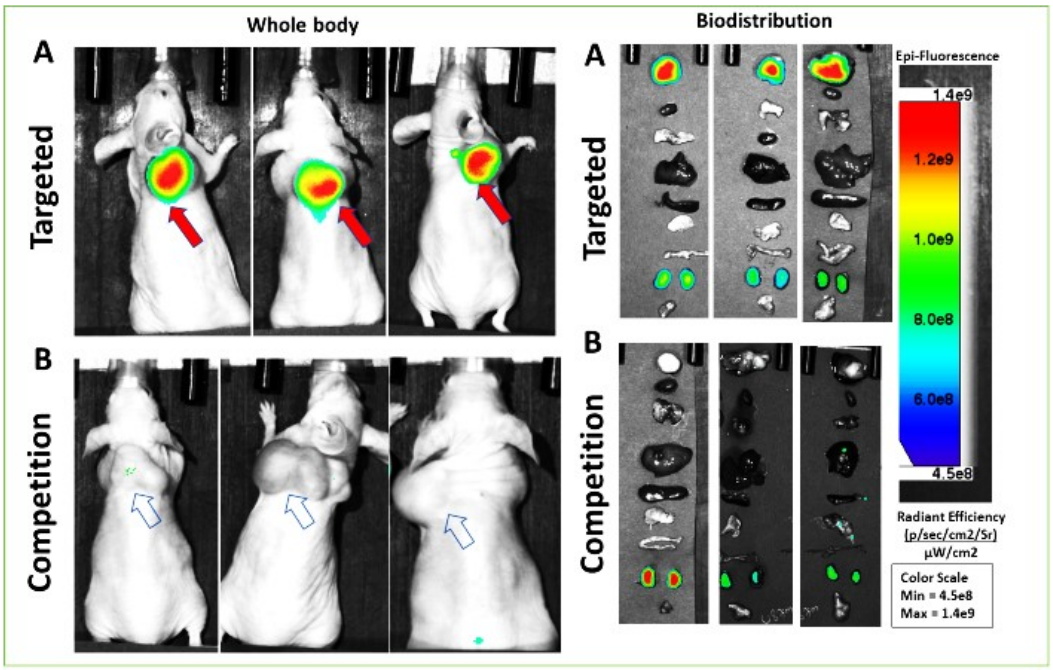

Fig. S6 In Vivo whole-body optical imaging and biodistribution of FTL-S-S0456 in U87Mg tumor bearing mice (n = 5). U87Mg tumor cells were implanted in female athymic nu/nu mice and tumors were allowed to grow to ~400 mm^3 prior to intravenous injection of 5 nmol FTL-S-S0456 (**4**) either in the absence (**A** both in whole body and biodistribution images) or presence (**B** both in whole body and biodistribution images) of excess FAP-ligand **3**. Two hours post injection mice were euthanized and imaged using an AMI imager. Mice from panels **A** and **B** were dissected and the biodistribution of FTL-S-S0456 is shown in the fluorescence images of panels **A** (targeted) and Panel **B** (competition). The tissues examined from top to bottom are tumor, heart, lungs, liver, spleen, stomach, small intestine, kidneys, and muscle.

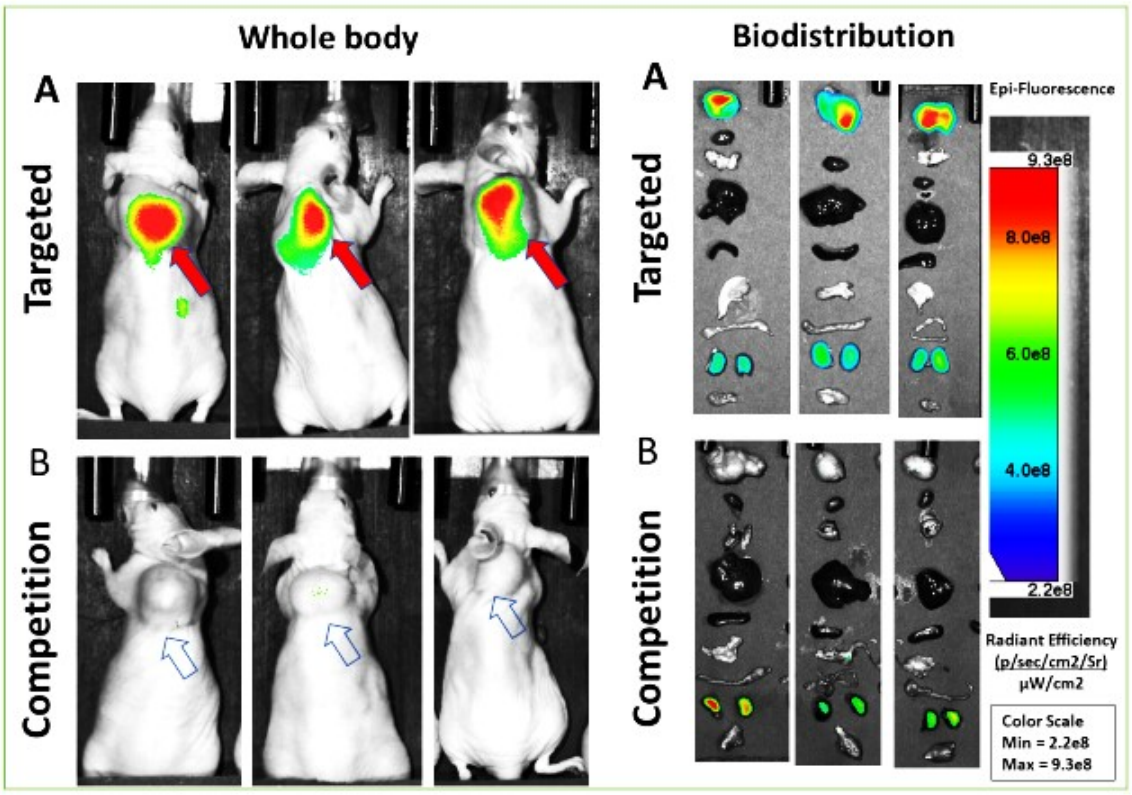

Fig. S7 In Vivo whole-body optical imaging and biodistribution of FTL-S-S0456 in FaDU tumor bearing mice (n = 5). FaDU tumor cells were implanted in female athymic nu/nu mice and tumors were allowed to grow to ~400 mm^3 prior to intravenous injection of 5 nmol FTL-S-S0456 (**4**) either in the absence (**A** both in whole body and biodistribution images) or presence (**B** both in whole body and biodistribution images) of excess FAP-ligand **3**. Two hours post injection mice were euthanized and imaged using an AMI imager. Mice from panels **A** and **B** were dissected and the biodistribution of FTL-S-S0456 is shown in the fluorescence images of panels **A** (targeted) and Panel **B** (competition). The tissues examined from top to bottom are tumor, heart, lungs, liver, spleen, stomach, small intestine, kidneys, and muscle.

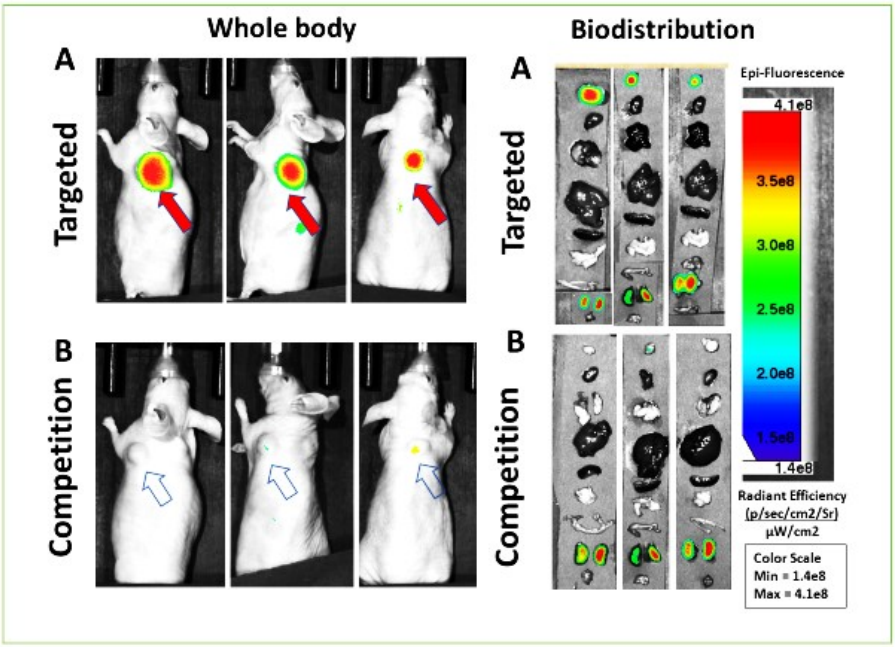

Fig. S8 In Vivo whole-body optical imaging and biodistribution of FTL-S-S0456 in PANC-1 tumor bearing mice (n = 5). PANC-1 tumor cells were implanted in female athymic nu/nu mice and tumors were allowed to grow to ~400 mm^3 prior to intravenous injection of 5 nmol FTL-S-S0456 (**4**) either in the absence (**A** both in whole body and biodistribution images) or presence (**B** both in whole body and biodistribution images) of excess FAP-ligand **3**. Two hours post injection mice were euthanized and imaged using an AMI imager. Mice from panels **A** and **B** were dissected and the biodistribution of FTL-S-S0456 is shown in the fluorescence images of panels **A** (targeted) and Panel **B** (competition). The tissues examined from top to bottom are tumor, heart, lungs, liver, spleen, stomach, small intestine, kidneys, and muscle.

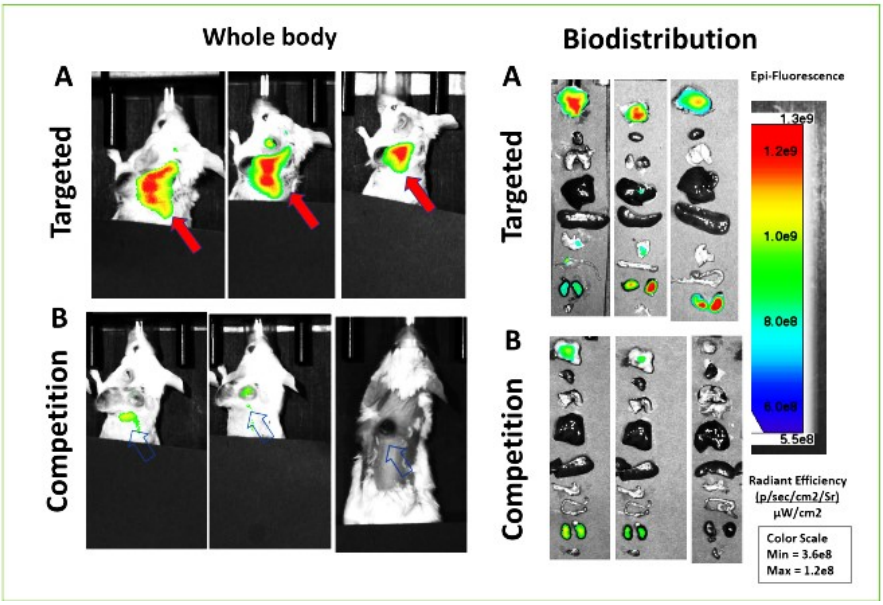

Fig. S9 In Vivo whole-body optical imaging and biodistribution of FTL-S-S0456 in 4T1 tumor bearing mice (n = 5). 4T1 tumor cells were implanted in female BALB/c mice and tumors were allowed to grow to ~400 mm^3 prior to intravenous injection of 5 nmol FTL-S-S0456 (**4**) either in the absence (A targeted**)** or presence (B competition) of excess FAP-ligand **3**. Two hours post injection mice were euthanized and imaged using an AMI imager. Mice from panels **A** and **B** were dissected and the biodistribution of FTL-S-S0456 is shown in the fluorescence images of panels **A** (targeted) and Panel **B** (competition). The tissues examined from top to bottom are tumor, heart, lungs, liver, spleen, stomach, small intestine, kidneys, and muscle.

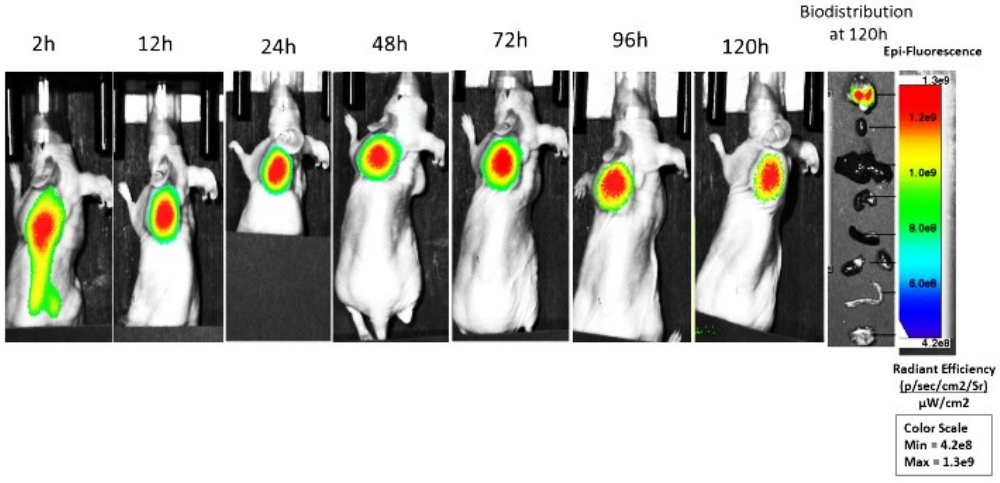

Fig. S10.Time course imaging study of FTL-S-S0456 to MDA-MB-231 cell tumors in athymic nu/nu mice. Analysis of the time course of uptake of FTL-S-S0456 in the aforementioned mice

implanted with FAP-negative MDA-MB-231 cells. The tissues examined from top to bottom are tumor, liver, lungs kidneys, intestine, stomach, and muscle.

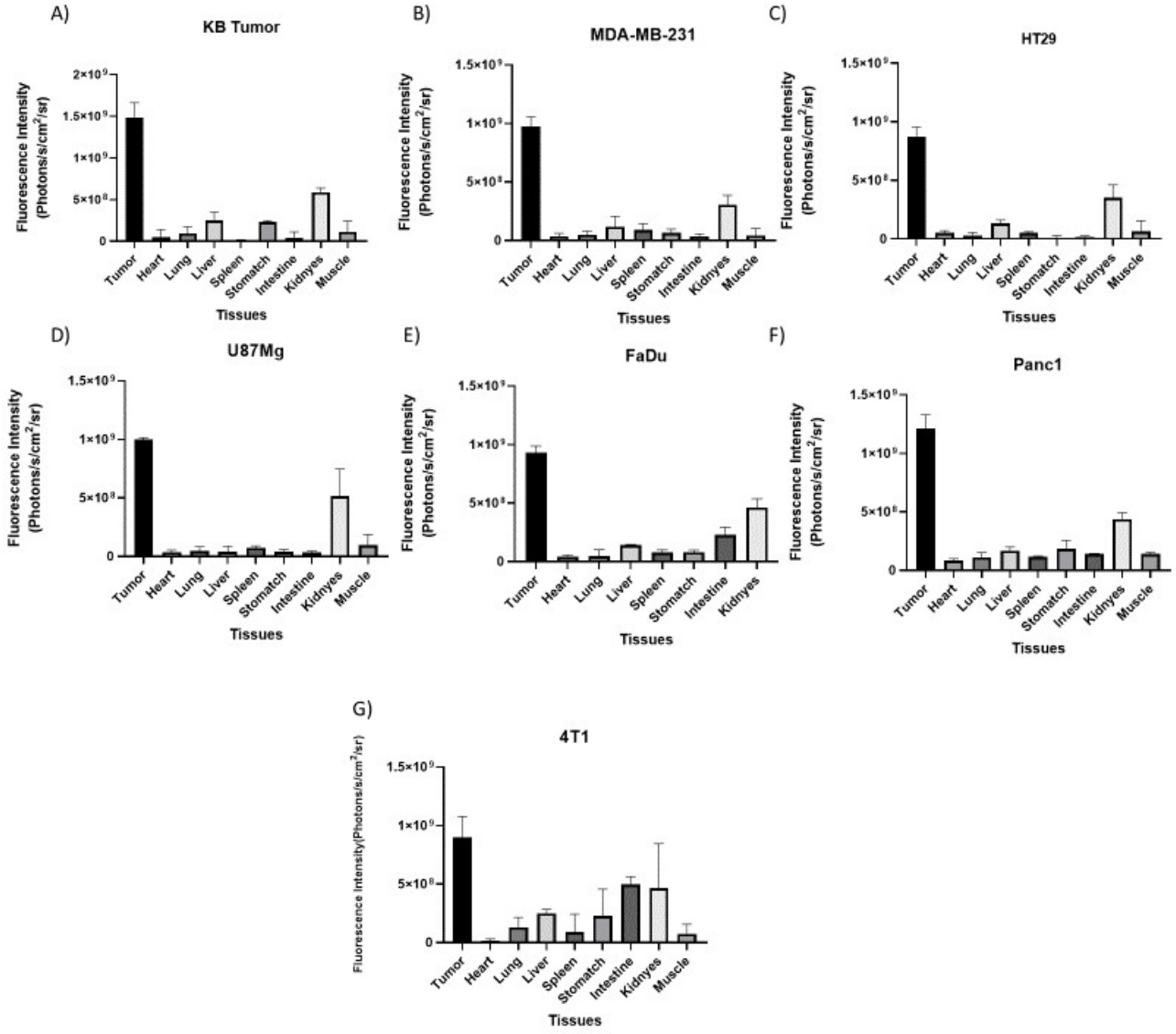

Fig.S11. Quantification of the fluorescence intensity of FTL-S-S0456 conjugate in A) KB, B) MDA-MB-231, C) HT29, D) U87Mg, E) FaDu, F) PANC-1 and G) 4T1 tumor-bearing mice. Mice were dosed with 5 nmol of FTL-S-S0456 via tail vein injection and euthanized and dissected 2 h post injection. Fluorescence intensities of major tissues and organs were determined using a AMI Fluorescence Imager. Data are mean ± SD of n = 3.

Molecular docking:

Protein Preparation:

The crystal structure of human fibroblast protein alpha [PDB ID: 1Z68] was obtained from the Protein Data Bank (www.rcsb.org) and further prepared for docking using the protein preparation toolbox included in the Schrodinger software package. The protein structure was preprocessed using the default protocol in Schrodinger and a pH value of 7.4 +/- 0.5 was used to generate heteroatomic states using the Epik module. The protein structure was further refined to optimize the intramolecular hydrogen bonds and a restrained energy minimization was performed using the OPLS4 force field.

Ligand preparation:

Structures of all three FAP ligands were uploaded into Maestro (Schrodinger, LLC, New York, NY, USA) and prepared for Glide docking using the LigPrep program in Schrodinger, LLC, NY, USA. Three-dimensional geometry of the ligand was optimized using the OPLS4 force field and used for docking.

Induced fit docking (IFD):

The standard Induced fit docking (IFD) protocol in the Schrodinger software package was used to dock the ligands of interest into the binding pocket of FAP. Firstly, a receptor grid box was generated by specifying the amino acid residues in FAP reported to be involved in binding interactions. The IFD protocol utilizes the Glide docking protocol to generate up to 20 poses for each ligand which are further refined using the Prime Refinement module. The residues within 5Å of ligand poses were refined and the side chains of the residues were optimized. Upon refinement of the binding site after initial docking, the ligands were redocked into structures that are within 30.0 kcal/mol of the best structure and within the top 20 structures overall. The standard precision model was used in the Glide redocking step.

Results:

Designing a drug conjugate requires careful choice of the linker attachment point so that the binding affinity of the modified drug remains similar to that of the parent drug. We have utilized molecular docking experiments to identify a suitable linker attachment point in the known inhibitor (**1**)[1]. In the docked pose of the inhibitor **1** with FAP, Glu204 and Tyr541 residues were found to be involved in non-covalent interactions, such that Glu204 forms a hydrogen bond with the N-H group of the pyrrolidine ring and Tyr541 forms a pi-pi interaction with the 2,3-dihydro isoindole ring of **1**. The shaded regions in the 2,3-dihydro isoindole ring mark the atoms that are solvent exposed (Fig. 1a). Based on this docking pose, we have hypothesized that the C-4 position of 2,3-dihydro isoindole ring in **1** can be further functionalized without compromising the conjugate's affinity for FAP**.** At first, we attached a methylene amine *(-CH_2NH_2)* at the C-4 position of the 2,3-dihydro isoindole ring and the resulting compound **1a** was docked with the FAP protein. The interactions of the modified ligand (**1a**) with the FAP protein were similar to those of the parent inhibitor **1** except that an additional cation-pi interaction in enabled between the 2,3-dihydro isoindole ring and Arg550. More importantly, the methylene amine (-CH_2NH_2) in **1a** was observed to remain solvent exposed for facile attachment of the spacer (Figure S12a). We observed the presence of nearby aromatic amino acid residues in the deep binding pocket of FAP and hypothesized that a hydrophobic spacer might help in forming some new stabilizing interactions with these aromatic amino acid residues. To test this hypothesis, methylene amine group in **1a** was replaced with a triazole ring containing a solvent exposed methylene amine (-CH_2NH_2) group (**1b**) which results in a pi-pi interaction of the triazole ring with Phe350. In the same orientation, the N-H of the methyl amine is predicted to form a hydrogen bond with Cys545 and the Arg123 is projected to form a hydrogen bond with the amide oxygen adjacent to the 2,3-dihydro isoindole ring (Figure S12b). This increased number of intermolecular interactions results in the increase of docking score from -8.0 kcal/mol to -9.4 kcal/mol. However, the purpose of inserting the triazole ring into the linker was initially to utilize it as a spacer for conjugation to drug conjugates. As the C-1 position *(-CH_2NH_2 unit*) of the triazole ring was found to be solvent exposed in the docking pose, we further replaced the methylene amine in **1b** with aminoethylbenzamide resulting in compound **1c** (Fig. 1b). We then docked **1c** with FAP and surprisingly found that it increased the docking score of **1c** to -11.5 kcal/mol, possibly because the phenyl ring in **1c** was found to form a pi-pi interaction with Trp623 and the 2,3-dihydro isoindole ring was seen to establish an additional

cation-pi interaction with Arg550 (Fig. 1b). The -NH_2 moiety in the **1c** was further utilized for attaching a PEG4-amine linker and the modified structure was docked again in the same binding pocket by setting up a larger grid box to accommodate the ligand-PEG4-amine drug conjugate (**2**). The interactions of the ligand with Glu204 and Tyr541 residues were conserved in the docked pose, and the docking score was calculated to be -9.5 kcal/mol (Fig. S12c). The triazole ring was involved in a pi-pi interaction with Phe350 like that shown in Fig. 1b. So, the docked poses of the modified ligand conjugates support our hypothesis that we were able to successfully add a spacer and a linker to the parent drug without interfering with the critical non-covalent interactions of the parent drug. Finally, the free amine functionality in compound **2** was utilized for synthesis of FAP targeted dye conjugate (**4)** as shown in scheme-2.

S12a

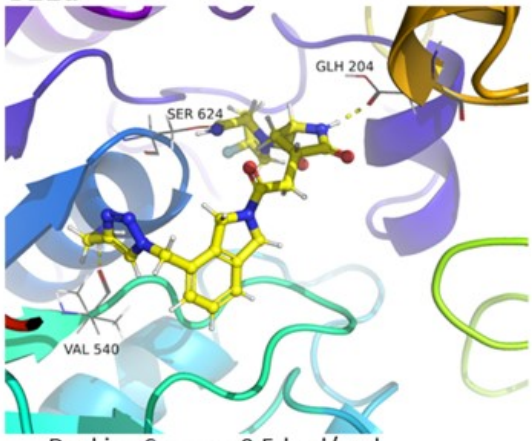

Docking Score = -9.5 kcal/mol

S12b

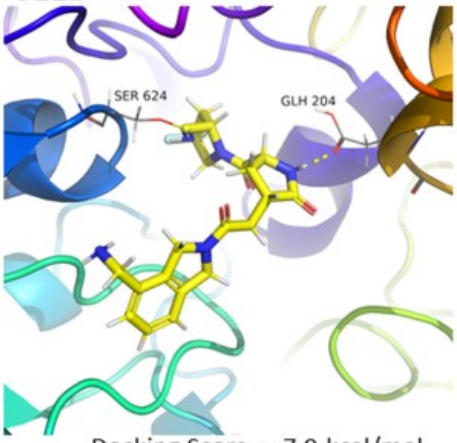

Docking Score = -7.9 kcal/mol

S12c

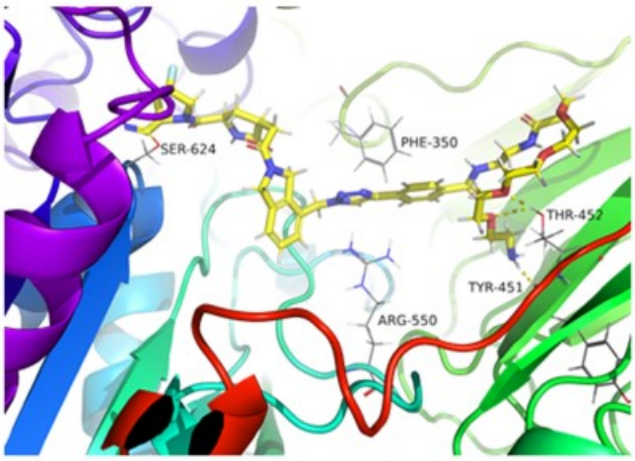

Docking Score = -9.1 kcal/mol

Figure S12a-c. 2D Ligand interaction diagram of (a-c) Compounds **1a-b** and **2** docked with human Fibroblast Activation Protein alpha (PDB ID: 1Z68).

Design and synthesis of a novel FAP-targeting ligand and its fluorescent conjugates.

Synthesis of FAP-targeted fluorescent conjugate **4** was then initiated from intermediates **5, 6** and **7** as shown in Scheme 1. Briefly, intermediate **5** was synthesized from commercially available Boc-L-pyroglutamic acid benzyl ester **8** as described in the literature[1]. Intermediate **6** was prepared from methyl 2,3-dihydro-1H-isoindole-4-carboxylate hydrochloride **9** by tert-butyloxycarbonyl (Boc) protection in dichloromethane to yield compound **10** in quantitative yield. The methyl ester in **10** was then reduced with $NaBH_4$ by heating in methanol and tetrahydrofuran to provide the corresponding alcohol **11** in 90% yield. Bromination of **11** with NBS/PPh_3 in DMF at room temperature followed by nucleophilic substitution of the corresponding bromide **12** with NaN_3 in DMF at 70 ^oC for 12h afforded the key azide intermediate **6** in 95% yield. Coupling of mono-Fmoc ethylenediamine hydrochloride with 4-ethynylbenzoic acid **13** in the presence of HATU/DIPEA in dry DMF yielded the alkyne intermediate **7**. The classical Cu(I)-catalyzed azide-alkyne cycloaddition (CuAAC) reaction of **6** with **7** in DMF at 55 ^oC for 5h then provided the click product **14** with the phenyl triazole appendage, and treatment of **14** with diethylamine in dichloromethane for 30 min, followed by coupling of the resultant amine with Fmoc-PEG_4-NHS ester in CH_2Cl_2 in the presence of DIPEA generated the intermediate **15** in 90% yield. Treatment of **15** with trifluoroacetic acid (TFA) in CH_2Cl_2 followed by coupling of the resultant amine with key acid intermediate **5** in the presence of HATU/DIPEA in DMF yielded the FAP-targeted ligand **16** in 65% yield (scheme -1).

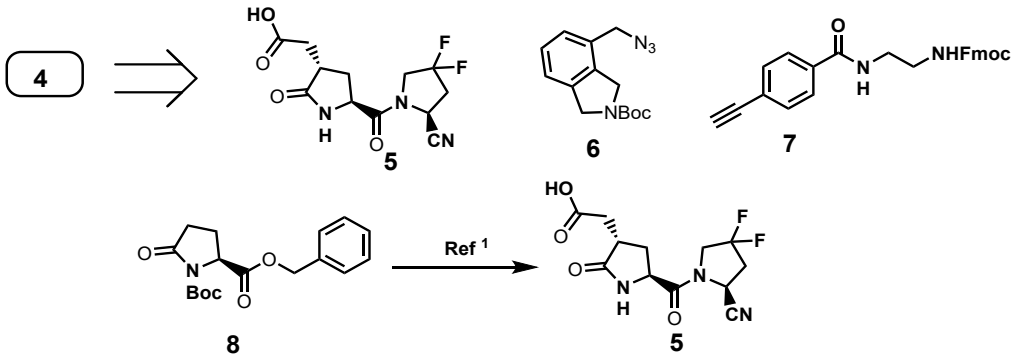

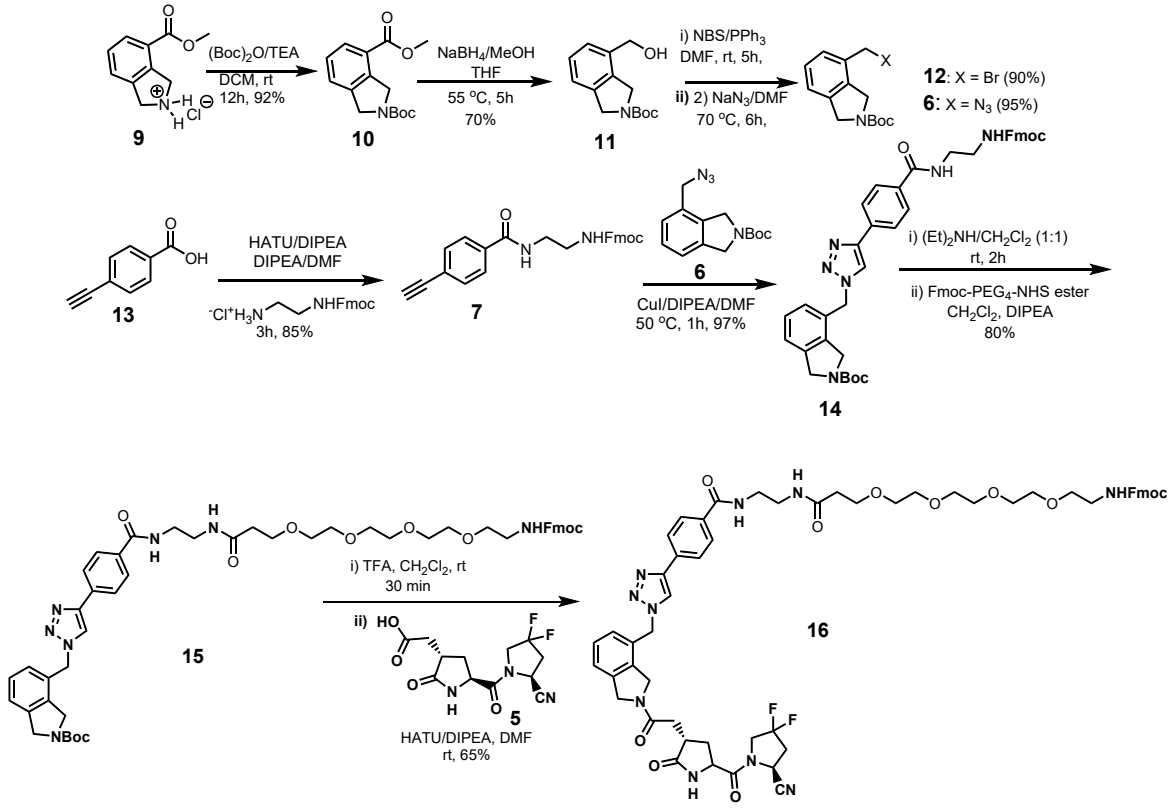

Scheme-1: Synthesis of key intermediates **5**, **6, 7** and **16.**

To generate the final FAP-targeted fluorescent dye used below, the Fmoc protecting group in **16** was deprotected with diethylamine in dichloromethane to generate the free amine **2**. Coupling of **2** with 3-(4-hydroxyphenyl) propionic acid followed by displacement of the chloride from the near infrared dye (ClS0456) under basic conditions provided the FAP-targeted near infrared dye (FTL-S-S0456) **4** in 65% yield (Scheme-2). Following synthesis, all intermediates and final products were characterized by liquid chromatography–mass spectrometry (LC-MS) and nuclear magnetic resonance spectroscopy (NMR), as described in the experimental section.

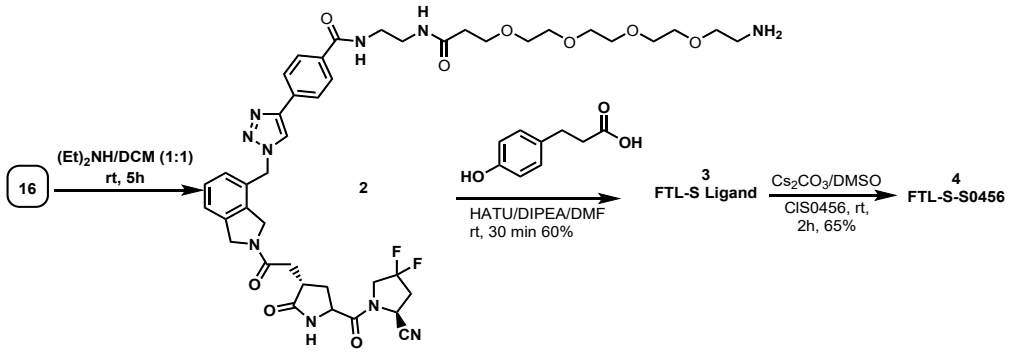

Scheme-2: Synthesis of FAP targeted fluorescent conjugate **4.**

Synthesis of 2-(tert-butyl) 4-methyl isoindoline-2,4-dicarboxylate (10): To a stirred solution of methyl 2,3-dihydro-1H-isoindole-4-carboxylate hydrochloride **9** (1.00 g, 5.64 mmol) in DCM (20 mL) at rt was added Add $(Boc)_2O$ (4.9 mL, 22.59 mmol) in one portion to the mixture followed by triethylamine (2.9 mL, 22.59 mmol) dropwise. Stirring was continued there for 12h, reaction mixture was diluted with water (30 mL) and extracted into DCM (2x25 mL), organic layer was dried over anhydrous MgSO4, filtered and filtrate was evaporated under reduced pressure and obtained crude residue was purified by combi flash using Hexanes + ethyl acetate as mobile phase provided the desired compound **10** (1.4g, 92% as white solid. ^{1}H-NMR ($CDCl_3$, 500 MHZ) δ = 7.92 (dd, J_1 = 15.0 Hz, J_2 = 10.0 Hz, 1H); 7.44-7.32 (m, 1H); 7.33 (m, 1H); 4.94 (d, J = 12.6 Hz, 2H); 4.67 (d, J = 17.0 Hz, 2H); 3.90 (s, 3H); 1.51 (s, 9H) ppm. ^{13}C-NMR ($CDCl_3$, 125 MHZ) δ = 166.41, 154.50, 154.33, 139.93, 138.96, 138.83, 138.56, 129.37, 128.96, 127.61, 127.17, 126.89, 125.55, 125.14, 79.80, 79.73, 53.80, 53.46, 52.05, 51.79, 51.49 28.55 ppm. LCMS for **4**: LC/MS (m/z): calcd for $C_{15}H_{21}NO_4$ $[M+H]^+$: 278.14, found 278.13g/mol.

Synthesis of tert-butyl 4-(hydroxymethyl)isoindoline-2-carboxylate (11):

To a stirred solution of compound **10** (1.0 g, 3.61 mmol) in THF (10.0 mL) at rt was added sodium borohydride (1.37 g, 36.101 mmol) in an atmosphere of nitrogen. Methanol (10 mL) was added to the above reaction mixture slowly for 5 minutes. The reaction was warmed to 55°C and stirring continued there for 5h. The reaction mixture was cooled to 0°C and slowly quenched with saturated aqueous ammonium chloride and extracted into EtOAc (60 mL). The organic phase was collected, dried over sodium sulfate and the solvent distilled to provide crude residue and which was purified by combi flash yielded the desired compound **11** (700 mg, 70%) as white gummy solid. ^{1}H-NMR ($CDCl_3$, 500 MHZ) δ = 7.28-7.25 (m, 2H); 7.19-7.13 (m, 1H); 4.68-4.62 (m, 6H); 1.51 (s, 9H) ppm. ^{13}C-NMR ($CDCl_3$, 125 MHZ) δ = 154.64, 137.60, 137.39, 135.62, 135.32, 143.92, 127.81, 125.90, 125.67, 122.05, 121.60, 79.87, 63.18, 62.80, 52.25, 51.95, 51.05, 50.81, 28.58, 28.54 ppm. LC-MS for **11.** LC-MS (m/z): calcd for $C_{14}H_{20}NO_3$ $[M+H]^+$: 250.14, found 250.14g/mol.

Synthesis of tert-butyl 4-(bromomethyl)isoindoline-2-carboxylate (12): To a stirred solution of alcohol **11** (500 mg, 2.00 mmol) in DMF (10 mL) was added PPh_3 (790 mg, 3.01 mmol) followed by freshly recrystallized N-bromosuccinimide (NBS) (532 mg, 3.01 mmol), stirred reaction mixture at rt under nitrogen atmosphere for 4 to 5 h. reaction mixture was diluted with

water (40 mL) followed by extracted into ethyl acetate (2x25 mL) organic layer was washed with water and brine followed by dried over anhydrous sodium sulphate, filtered and filtrate was evaporated under reduced pressure and obtained crude residue was purified by combi flask provided the bromo compound **12** (450 mg, 90%) as white solid. ^{1}H-NMR ($CDCl_3$, 500 MHZ) δ = 7.28-7.17 (m, 3H); 4.71 (m, 4H); 4.42 (d, J = 8.5 Hz, 2H); 1.52 (s, 9H) ppm. ^{13}C-NMR ($CDCl_3$, 125 MHZ) δ = 154.46, 138.38, 138.03, 136.78, 136.48, 132.44, 132.17, 128.20, 128.13, 127.8, 123.18, 122.90, 79.98, 79.88, 52.4, 52.18, 50.74, 50.63, 28.58, 28.54 ppm. LC-MS for **12**: LC-MS: (m/z):calcd for $C_{14}H_{19}BrNO_2$ $[M+H]^+$: 312.05, found 312.05 g/mol.

Synthesis of tert-butyl 4-(azidomethyl)isoindoline-2-carboxylate (6): To a stirred solution bromide **12** (400 mg, 1.286 mmol) in DMF was added NaN_3 (420 mg, 6.430 mmol), then stirring continued at 75 ^{o}C for 6h. Reaction mixture was diluted with water and extracted into ethyl acetate, organic layer was washed with water, brine and dried over anhydrous sodium sulphate, filtered and filtrate was evaporated under reduced pressure and purified by combi flask gave azide **6** (300 mg, 95%) as white solid**.** ^{1}H-NMR ($CDCl_3$, 500 MHZ) δ = 7.32-7.25 (m, 2H); 7.22-7.20 (m, 1H); 4.72-4.66 (m, 4H); 4.31 (s, 2H); 1.53 (s, 9H) ppm. ^{13}C-NMR ($CDCl_3$, 125 MHZ) δ = 154.42, 138.28, 137.95, 136.34, 135.95, 130.18, 129.92, 128.08, 127.40, 127.30, 122.96, 122.65, 79.96, 52.59, 52.48, 52.39, 52.15, 51.05, 50.89, 28.56 ppm. LC-MS for **7**: LC-MS (m/z): calcd for $C_{14}H_{19}N_4O_2$ $[M+H]^+$: 275.14, found 275.14 g/mol.

Synthesis of (9H-fluoren-9-yl)methyl (2-(4-ethynylbenzamido)ethyl)carbamate (7): To a stirred solution of 4-Ethynylbenzoic acid **13** (500 mg, 3.424 mmol) in dry DMF (10 mL) at room temperature under nitrogen atmosphere was added HATU (1.4 gm, 3.76 mmol) followed by DIPEA (1.7 mL, 10.27m mol) and stirring continued there for 10 min for activation of acid. N-Fmoc-ethylenediamine (1.0 g, 3.76 mmol) was added to the reaction mixture and continued stirring for additional 3h. reaction mixture was diluted with water (50 mL) and obtained precipitate was filtered through Buckner funnel and resulting white solid was wash with water (2x50 mL) again and dried under vacuum for 1h provided coupled product **7** (1.2gm, 85%): ^{1}H-NMR (CD_3OD +$CDCl_3$, 500 MHZ) δ = 7.76-7.73 (m, 4H); 7.59 (d, J = 7.5 Hz, 2H); 7.50 (d, J = 8.3 Hz, 1H); 7.35 (t, J = 7.4 Hz, 2H); 7.25 (m, 2H); 4.44 (bs, 2H); 4.33 (d, J = 7.0 Hz, 1H); 4.16 (t, J = 7.0 Hz, 1H); 3.50 (s, 1H); 3.48 (t, J = 6.1Hz, 2H); 3.34(t, J = 6.0 Hz, 2H) ppm. ^{13}C-NMR (CD_3OD +$CDCl_3$, 125 MHZ) δ = 168.27, 158.16, 143.81, 141.20, 134.02, 131.83, 127.49, 127.06, 126.85, 125.62,

124.83, 119.65, 83.34, 79.69, 77.92, 66.61, 47.06,40.04 ppm. and LC-MS for **7**: LC-MS (m/z): calcd for $C_{26}H_{23}N_2O_3$ [M+H]: 411.16, found 411.16 g/mol. HRMS-ESI: calcd for $C_{26}H_{23}N_2O_3$ [M + H]$^+$: 411.1708, found 411.1710

Synthesi of tert-butyl4-((4-(4-((2-((((9H-fluoren-9-yl)methoxy)carbonyl)amino)ethyl) carbamoyl) phenyl) -1H-1,2,3-triazol-1-yl)methyl)isoindoline-2-carboxylate (14) : To a mixture of azide **6** (1.0 eq) and alkyne **7** (1.2 eq) in dry DMF (5.0 mL) was added CuI (0.5 eq) followed by DIPEA (2.0 eq). Reaction mixture was stirred at 55 ^oC, under nitrogen atmosphere for 1h, transfer the reaction mixture to room temperature and diluted with saturated aqueous ammonium chloride (20 mL) and vigorously stirred there for 15 min, solid residue formed in the reaction mixture was filtered and washed with water 2x20 mL, dried under vacuum for 1h provide the desired compound **14** as brown solids and this was taken to further step without purification or also purify it using EtOAC/Hexanes mixture as mobile phase provided desired compound **14** as white solid (97%). ^{1}H-NMR ($CDCl_3$, 500 MHZ) δ = 7.79 (bs, 3H); 7.78-7.70 (m, 2H); 7.68 (d, J = 7.9 Hz, 2H); 7.52 (d, J = 7.3 Hz, 2H); 7.73-7.720 (m, 7H); 7.15-7.13 (m, 1H); 5.50 (s, 2H); 4.67-4.57 (m, 4H); 4.34 (d, J = 6.7 Hz, 2H); 4.12 (t, J = 6.7 Hz, 1H); 3.48 (t, J = 5.7 Hz, 1H); 3.35-3.33 (m, 2H); 2.77 (s, 2H); 2.71 (bs, 1H); 1.46 (s, 9H) ppm. ^{13}C-NMR ($CDCl_3$, 125 MHZ) δ = 173.47, 167.26, 156.65, 154.33, 144.98, 141.27, 138.65, 138.46, 136.59, 135.92, 129.26, 129.03, 128.58, 127.82, 127.67, 127.44, 127.06, 125.61, 125.12, 123.58, 123.26, 119.95, 80.18, 80.08, 70.49, 70.13, 67.14, 66.58, 50.98, 50.80, 47.25, 40.91, 39.06, 36.85, 28.52 ppm. LC-MS for **14:** LC-MS (m/z): calcd for $C_{40}H_{41}N_6O_5$ [M+H]$^+$: 685.31, found 685.31g/mol. HRMS-ESI: calcd for $C_{40}H_{41}N_6O_5$ [M + H]+ : 685.3138, found 685.3139.

Synthesis of tert-butyl 4-((4-(4-((1-(9H-fluoren-9-yl)-3,19-dioxo-2,7,10,13,16-pentaoxa-4,20-diazadocosan-22-yl)carbamoyl)phenyl)-1H-1,2,3-triazol-1-yl)methyl)isoindoline-2-carboxylate (15):

To a stirred solution compound **14** (400mg, 0.584 mmol) in DCM+MeOH Mixture (1+0.5 mL) was added $(Et)_2NH$ (1.0 mL) and stirring continued there for 2h. reaction mixture was evaporated under reduced pressure and obtained crude residue purified combi flash using MeOH +CH_2Cl_2 as mobile provided the free amine of compound **14** and which was used for further step. The amine compound was dissolved in DCM (1 mL for 1mmol) followed by Fmoc-NH$(PEG)_4$ NHS ester (1.2 eq) and DIPEA (2.0 eq) were added and stirred the reaction mixture at rt, under nitrogen

atmosphere for 1h, reaction mixture evaporated under reduced pressure and obtained crude residue was purified by combi flash using DCM +MeOH as mobile phase provide the compound **15** in 80% as white solid.

^{1}H-NMR ($CDCl_3$, 500 MHZ) δ = 7.86 (m, 4H); 7.74 (d, J = 7.5 Hz, 2H);7.68 (d, J = 3.7 Hz, 1H); 7.57 (m, 3H); 7.37 (t, J = 7.5 Hz, 2H); 7.28 (m, 4H); 7.16 (m, 2H); 5.67 (bs, 1H); 5.51 (d, J = 6.7 Hz, 2H); 4.71 (s, 2H); 4.65 (m, 2H); 4.37 (d, J = 7.2Hz, 1H); 4.19 (t, J = 7.0 Hz, 1H); 3.72-3.34 (m, 22H); 2.44 (s, 2H); 1.51 (s, 9H) ppm. **^{13}C-NMR ($CDCl_3$, 125 MHZ) δ** = 173.47, 167.26, 156.65, 154.33, 143.98, 141.27, 138.65, 138.46, 136.59, 135.92, 133.77, 133.19, 129.26, 129.03, 128.58, 127.82, 127.67, 127.44, 127.06, 125.61, 125.12, 123.58, 123.26, 119.95, 80.18, 80.08, 70.49, 70.42, 70.13, 70.06, 67.14, 66.58, 52.11, 51.92, 51.73, 50.90, 50.81, 47.25, 41.59, 40.90, 39.06, 36.85, 28.52 ppm. LC-MS for **15**:LC-MS (m/z): calcd for $C_{51}H_{62}N_7O_{10}$ $[M+H]^+$: 932.45, found 932.45g/mol. HRMS-ESI: calcd for $C_{51}H_{61}N_7O_{10}Na$ $[M + Na]^+$: 954.4377, found 954.4433.

Synthesis of (9H-fluoren-9-yl)methyl (1-(4-(1-((2-(2-((3S)-5-((S)-2-cyano-4,4-difluoropyrrolidine-1-carbonyl)-2-oxopyrrolidin-3-yl)acetyl)isoindolin-4-yl)methyl)-1H-1,2,3-triazol-4-yl)phenyl)-1,6-dioxo-9,12,15,18-tetraoxa-2,5-diazaicosan-20-yl)carbamate (16):

To a stirred solution of compound **15** (250 mg, 0.268 mmol) in DCM (1.0 mL) at rt, was added TFA (0.5 mL) and stirring was continued there for 30 min. reaction mixture was evaporated and dried under vacuum. In a separate round bottom flask acid **5** (100 mg, 0.333 mmol) was dissolved in DMF (0.5 mL) followed by HATU (151 mg, 0.399 mmol), DIPEA (0.170 mL, 0.999mmol) and reaction mixture stirred under nitrogen atmosphere at rt for 10 min for activation of acid functionality. The amine in situ generated from **15** (220 mg, 0.268 mmol) was dissolved in DMF (1 mL) added to above reaction mixture and continued stirring there 2h, reaction mixture was diluted with water (15 mL) and stirred at rt for 15 min, the black turbidity formed in the reaction mixture was filtered followed by redissolved in the mixture of methanol+dichloromethane , evaporated the organic layer and obtained crude residue was purified reversphase preparative high performance liquid chromatography (HPLC) (A= 20 mm ammonium acetate buffer (pH = 7), B = acetonitrile, solvent gradients 5% B to 95% in 60 min provided the compound **16** as white solid (175 mg, 65%). ^{1}H-NMR (CD_3OD + $CDCl_3$, 500 MHZ) δ = 8.32 (d, J= 15.0 Hz, 1H), 7.89-7.85 (m, 4H), 7.73 (d, J = 10.0 Hz, 2H); 7.58 (d, J = 5.0 Hz, 2H); 7.35-7.24 (m, 8H); 5.61-5.59 (m, 2H);

5.05 (dd, J1 = 9.1 Hz, J2 = 3.9 Hz, 1H); 4.85 (m, 2H); 4.72 (d, J = 17.2Hz, 2H); 4.45-4.37 (m, 1H); 4.31 (d, J = 6.8 Hz, 2H); 4.15-4.02 (m, 3H); 3.67 (t, J = 6.0 Hz, 2H); 3.55-3.48 (m, 20H); 3.31-3.25 (m, 6H); 3.0-2.74 (m, 5H); 2.60-2.54 (m, 1H); 2.43-2.30 (m, 4H) ppm. ^{13}C-NMR (CD_3OD + $CDCl_3$, 125 MHZ) δ = 173.28, 168.36, 156.66, 143.88, 141.19, 127.76, 127.45, 126.83, 125.34, 124.82, 121.72, 119.62, 70.72, 70.19, 69.99, 69.91, 69.62, 66.85, 66.30, 52.80, 52.06, 44.58, 40.44, 39.86, 38.69, 37.60 36.38 ppm. LC-MS for **16**: LC-MS (m/z): calcd $C_{58}H_{65}F_2N_{10}O_{11}$ $[M+H]^+$: 1115.47, found 1115.47 g/mol. HRMS-ESI: calcd for $C_{58}H_{65}F_2N_{10}O_{11}$ $[M+H]^+$: 1115.4802, found 1115.4817.

Synthesis of 5-((1-(4-(1-((2-(2-((3S,5S)-5-((S)-2-cyano-4,4-difluoropyrrolidine-1-carbonyl)-2-oxopyrrolidin-3-yl)acetyl)isoindolin-4-yl)methyl)-1H-1,2,3-triazol-4-yl)phenyl)-1,6-dioxo-9,12,15,18-tetraoxa-2,5-diazaicosan-20-yl)carbamoyl)-2-(6-(dimethylamino)-3-(dimethyliminio)-3H-xanthen-9-yl)benzoate (4):

To a stirred solution of compound **16** (250.0 mg, 0.2244 mmol) in DCM +MeOH (1+1 mL) was added diethyl amine $(Et)_2NH$ (2.0 mL) and continued stirring at rt for 2h, reaction mixture was evaporated under reduced pressure, obtained crude residue was re dissolved in EtOAc (10 mL) and resulted precipitate was d filtered through Buckner funnel to provided free anime (**2**) as brown solid, LC-MS for **2:** LC-MS (m/z): calcd for $C_{43}H_{55}F_2N_{10}O_9$ $[M+H]^+$: 893.40, found 893.40 g/mol (Fig.S24). HRMS-ESI: calcd for $C_{43}H_{55}F_2N_{10}O_9$ $[M+H]^+$: 893.4121, found 893.4160. This material further used for synthesis of final FAP targeted dye conjugate **4** as described below.

Synthesis of 4-(1-((2-(2-((3S,5S)-5-((S)-2-cyano-4,4-difluoropyrrolidine-1-carbonyl)-2-oxopyrrolidin-3-yl)acetyl)isoindolin-4-yl)methyl)-1H-1,2,3-triazol-4-yl)-N-(22-(4-hydroxyphenyl)-4,20-dioxo-7,10,13,16-tetraoxa-3,19-diazadocosyl)benzamide (3):

To a stirred solution of amine **2** (50 mg, 0.056 mmol) in DMF (1.0 mL) were added. 3-(4-Hydroxyphenyl) propionic acid (14.0 mg, 0.084 mmol), HATU (38.0 mg, 0.101 mmol) and DIPEA (42 µl, 0.252 mmol). continued stirring at rt for 30 min and reaction mixture was quenched by water (5 mL) and obtained crude residue was purified by using UHPLC (A = 20 Mm ammonium acetate buffer (pH = 7), B = acetonitrile, solvent gradients 5% B to 95% in 60 min provided the desired compounds **3** as white solid (34 mg, 60%). LC/MS for **3**: LC-MS (m/z): calcd for $C_{52}H_{63}F_2N_{10}O_{11}$ $[M+H]^+$: 1041.46, found: 1041.46. HRMS-ESI: calcd for $C_{52}H_{63}F_2N_{10}O_{11}[M+H]^+$: 1041.4645, found 1041.4650.

Synthesis of sodium 2-((E)-2-((E)-2-(4-(1-(4-(1-((2-(2-((3S,5S)-5-((S)-2-cyano-4,4-difluoropyrrolidine-1-carbonyl)-2-oxopyrrolidin-3-yl)acetyl)isoindolin-4-yl)methyl)-1H-1,2,3-triazol-4-yl)phenyl)-1,6,22-trioxo-9,12,15,18-tetraoxa-2,5,21-triazatetracosan-24-yl)phenoxy)-3-(2-((E)-3,3-dimethyl-5-sulfonato-1-(4-sulfonatobutyl)indolin-2-ylidene)ethylidene)cyclohex-1-en-1-yl)vinyl)-3,3-dimethyl-1-(4-sulfonatobutyl)-3H-indol-1-ium-5-sulfonate (4):

To a stirred solution of **3** (5.0 mg, 0.00480 mmol) in anhydrous DMSO (500 µl) at rt under argon atmosphere was added ClS0456 Dye (4.6 mg, 0.0048 mmol) followed by Cs_2CO_3 (15.0 mg, 0.0480 mmol) and continued stirring there for additional 3 h to 4h, progress of the reaction was monitored by LCMS. Reaction mixture was diluted with water and purified by using UHPLC (A = 20 Mm ammonium acetate buffer (pH = 7), B =0 acetonitrile, solvent gradients 5% B to 35% in 60 min provided desired compound 5 as fluffy green solid (6.0 mg, 66%). LC-MS for **4:** LC/MS (m/z): [M+H] calcd for $C_{90}H_{110}F_2N_{12}O_{23}S_4$ [M+H]+: 1892.66, found: 1892.65, $[M+H]^{+2}$: 946.9, and $[M+H]^{+3}$: 631.6 g/mol. HRMS-ESI: calcd for $C_{90}H_{109}F_2N_{12}O_{23}S_4$ $[M^+]$: 1891.6593, found: 1891.6515, $[M+H]^{+2}$ **:** 946.3323 and $[M+H]^{+3}$: 631.2238. **^{1}H-NMR (D_2O, 500 MHZ)** δ = 8.27 (m, 1H); 7.62 (m, 10H); 7.12 (d, J = 6.2Hz, 5H); 6.97 (dd, J = 14.7 Hz, 7.9 Hz, 2H); 6.64 (dd, J = 14.1 Hz, 8.1 Hz, 2H); 5.86 (dd, J = 14.3 Hz, 3H); 5.40 (d, J = 9.8 Hz, 3H);4.97 (m, 3H); 4.54 (d, J = 7.5 Hz, 3H); 4.46 (s, 1H); 4.35 (s, 1H); 3.97 (m, 1H); 3.85 (s, 6H); 3.50 (s, 6H); 3.26 (m, 20H); 3.09 (m, 3H); 2.77(s, 10H); 2.62 (m, 4H); 2.33 (m,9H); 2.15 (m, 2H); 1.90 (d, J = 0.9 Hz, 7H); 1.68 (s, 10 H); 0.95 (s, 10 H) ppm.

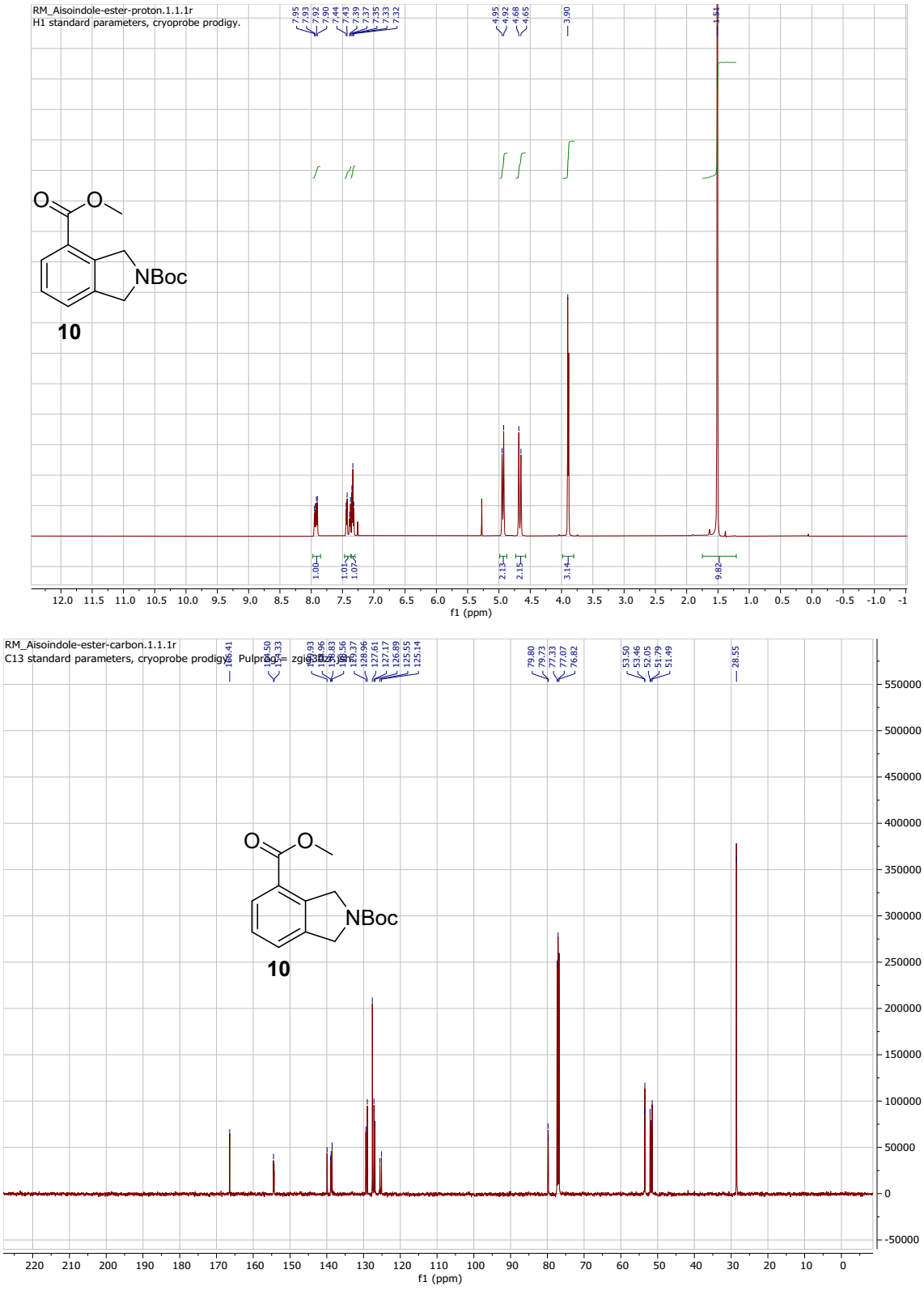

Fig. S13: ^{1}H &^{13}C NMR spectra of compound **10**

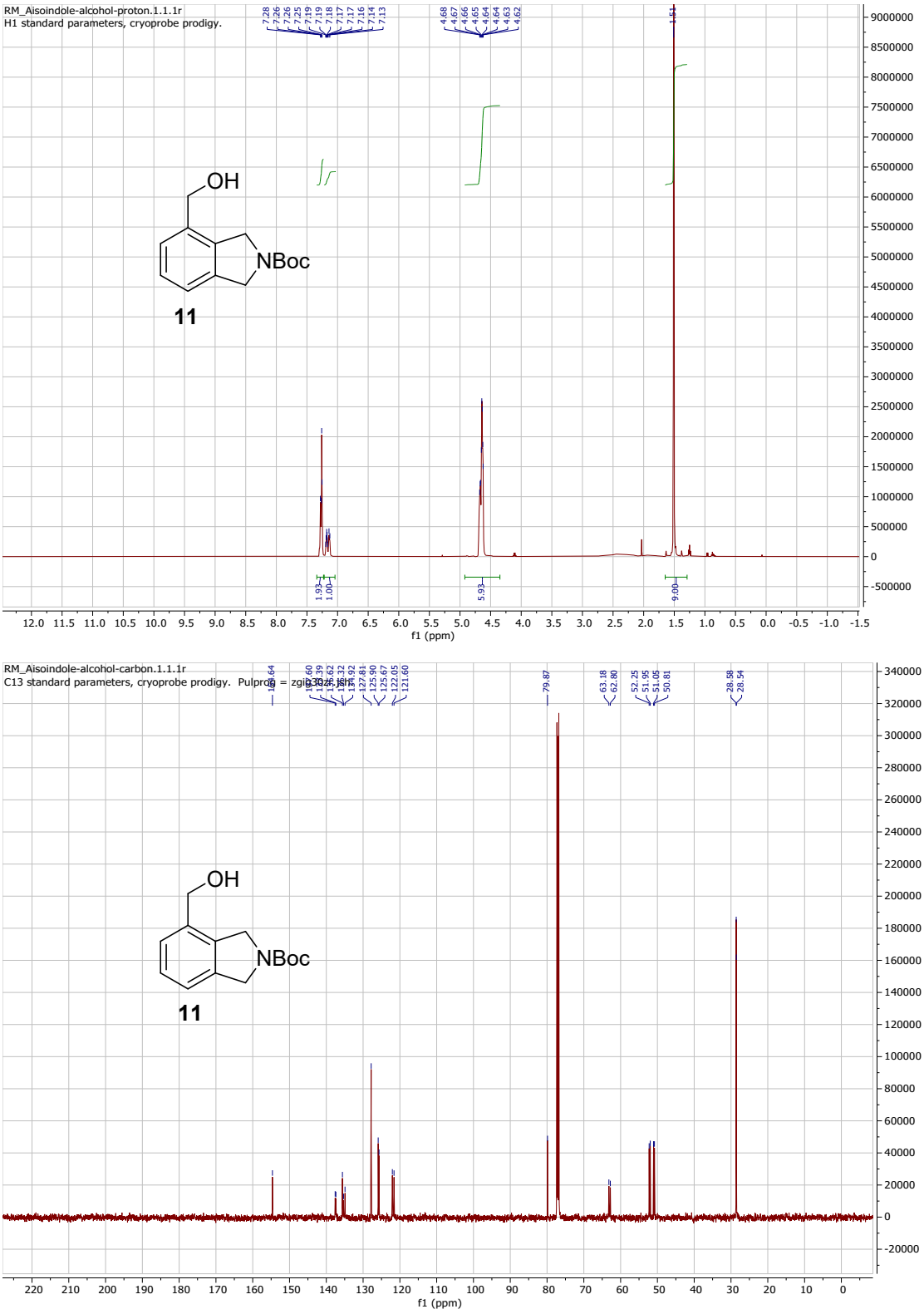

Fig. S14: ^{1}H &^{13}C NMR spectra of compound **11**

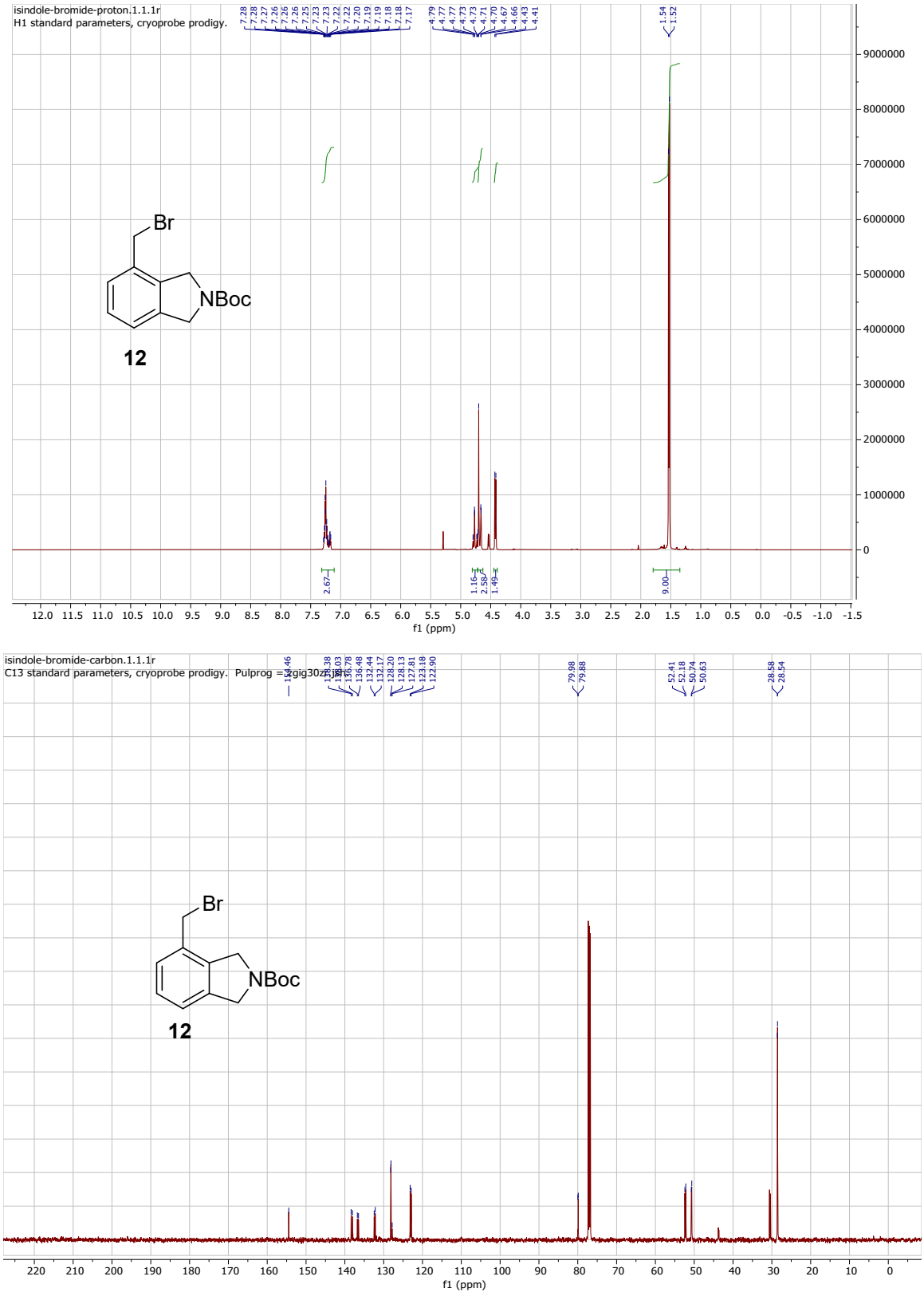

Fig. S15: ^{1}H &^{13}C NMR spectra of compound **12**

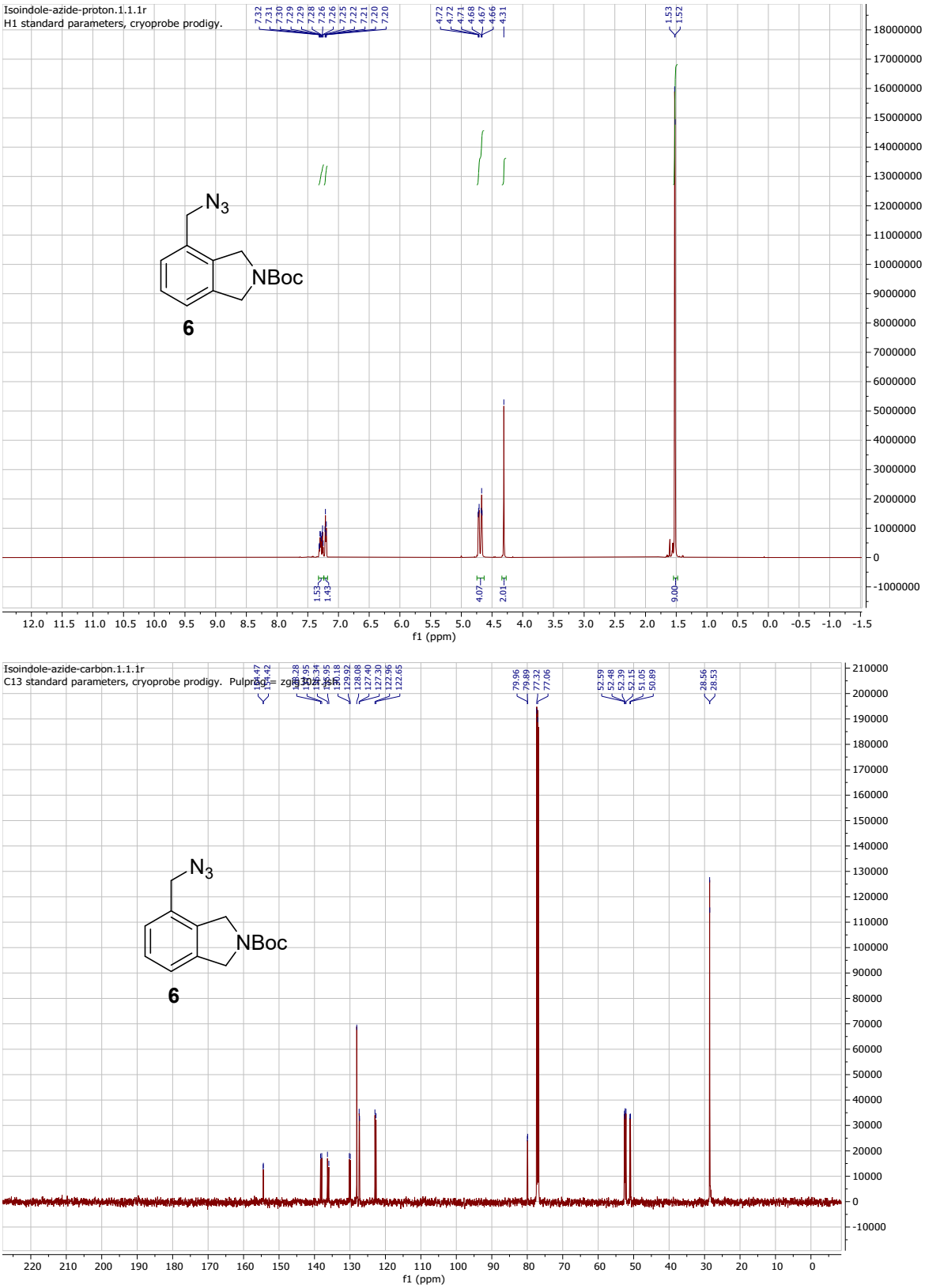

Fig. S16: ^{1}H &^{13}C NMR spectra of compound **6**

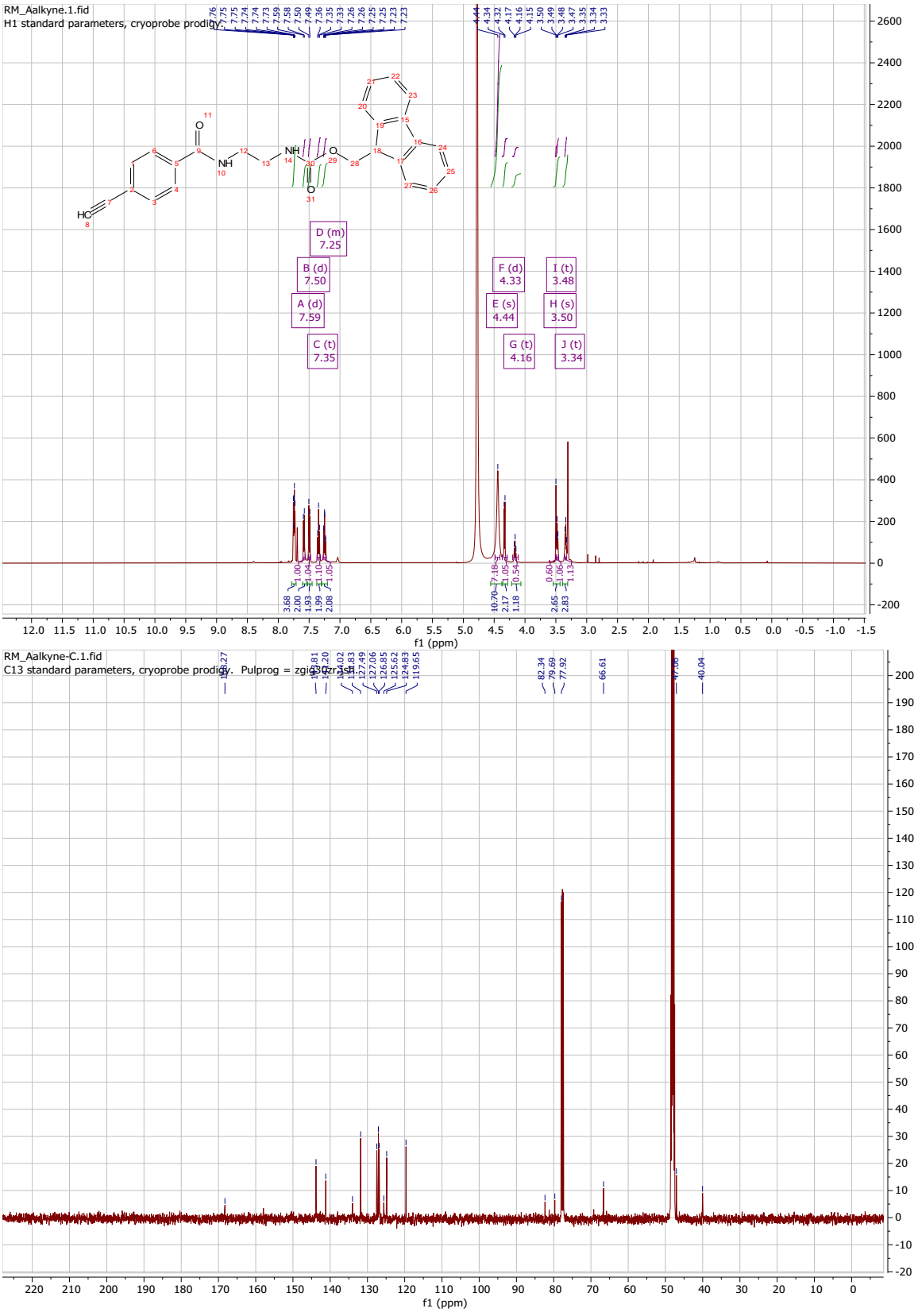

Fig. S17: ^{1}H &^{13}C NMR spectra of compound **13**

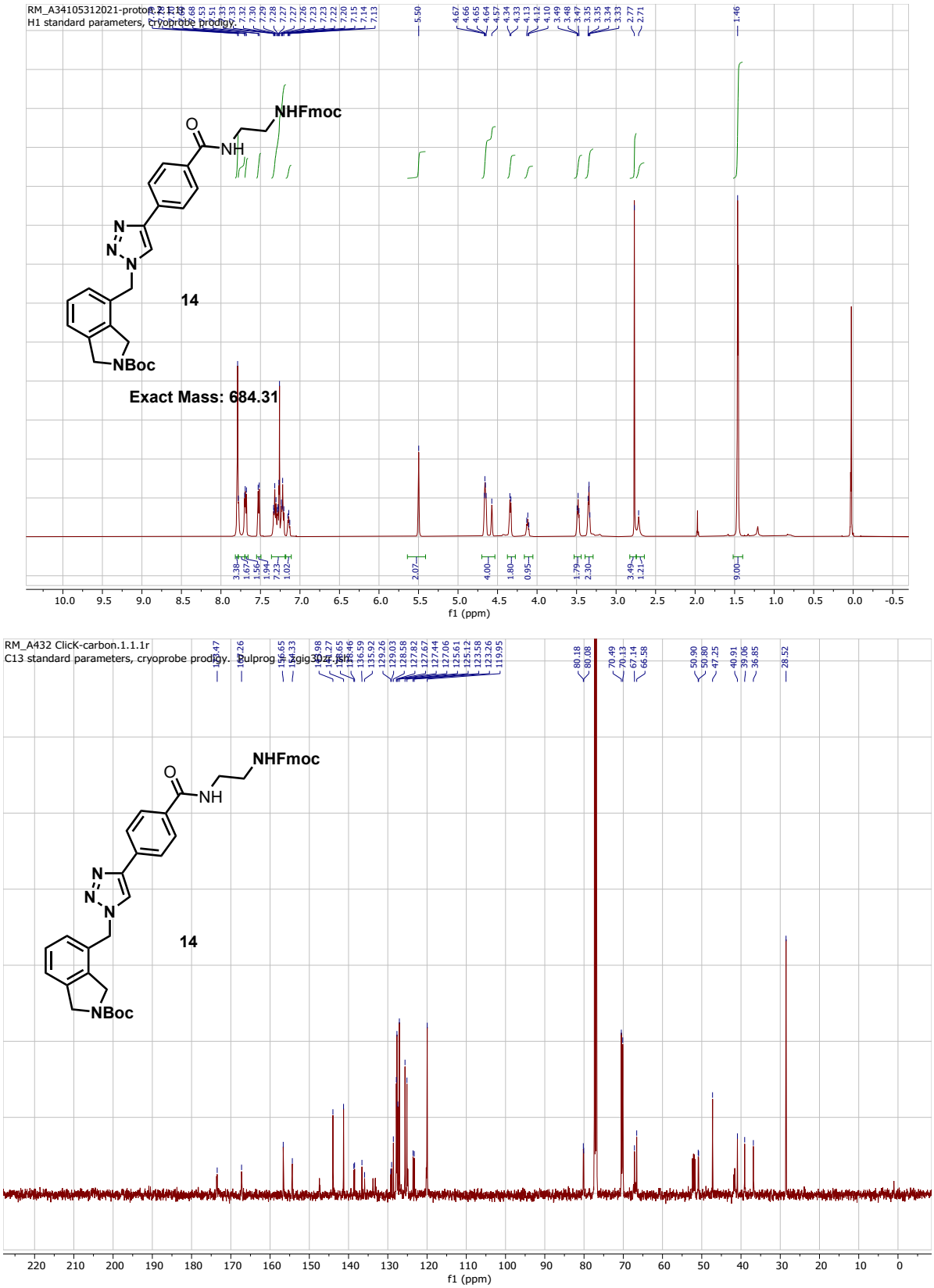

Fig. S18: ^{1}H &^{13}C NMR spectra of compound **14**

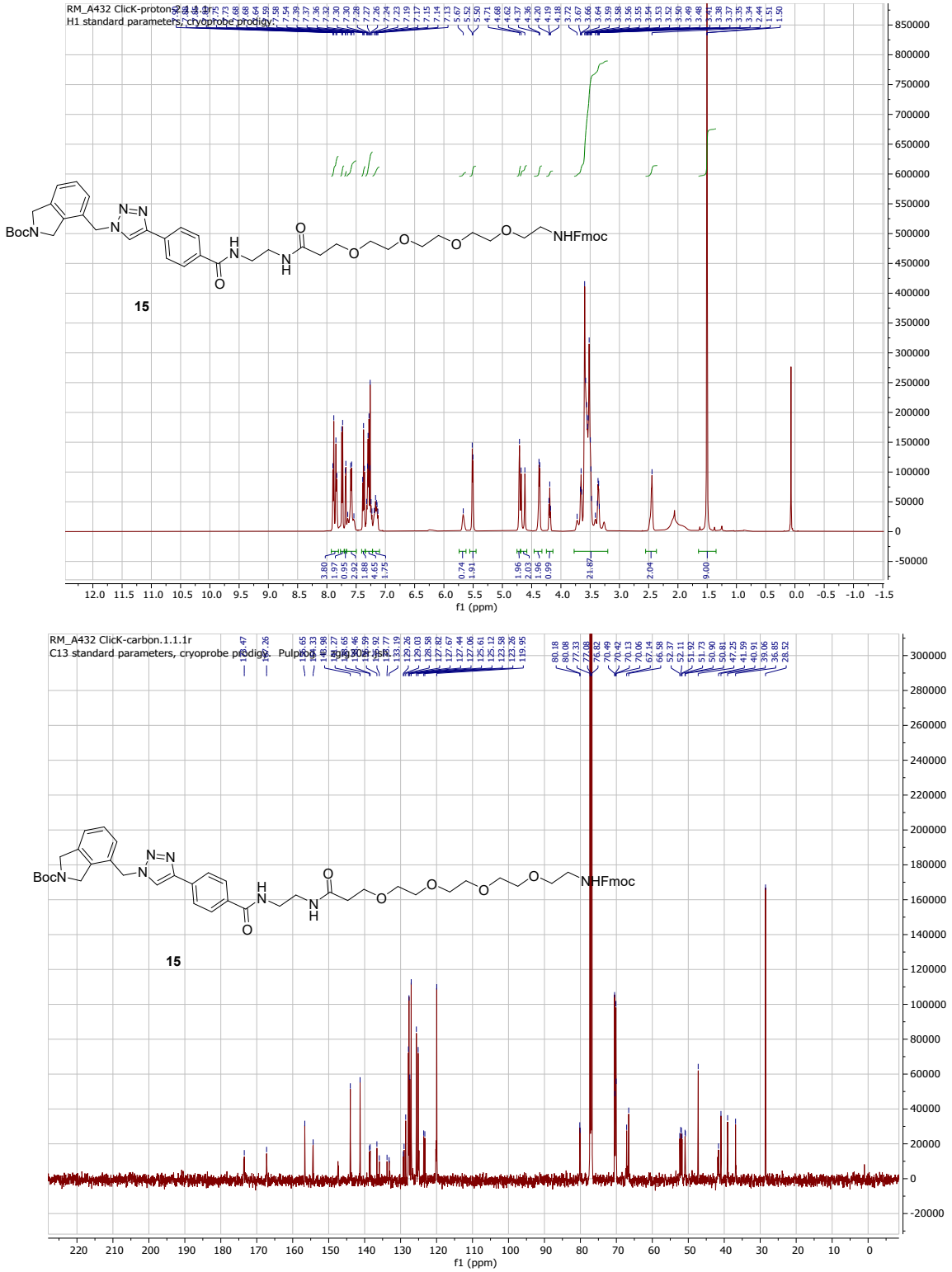

Fig. S19: ^{1}H &^{13}C NMR spectra of compound **15**

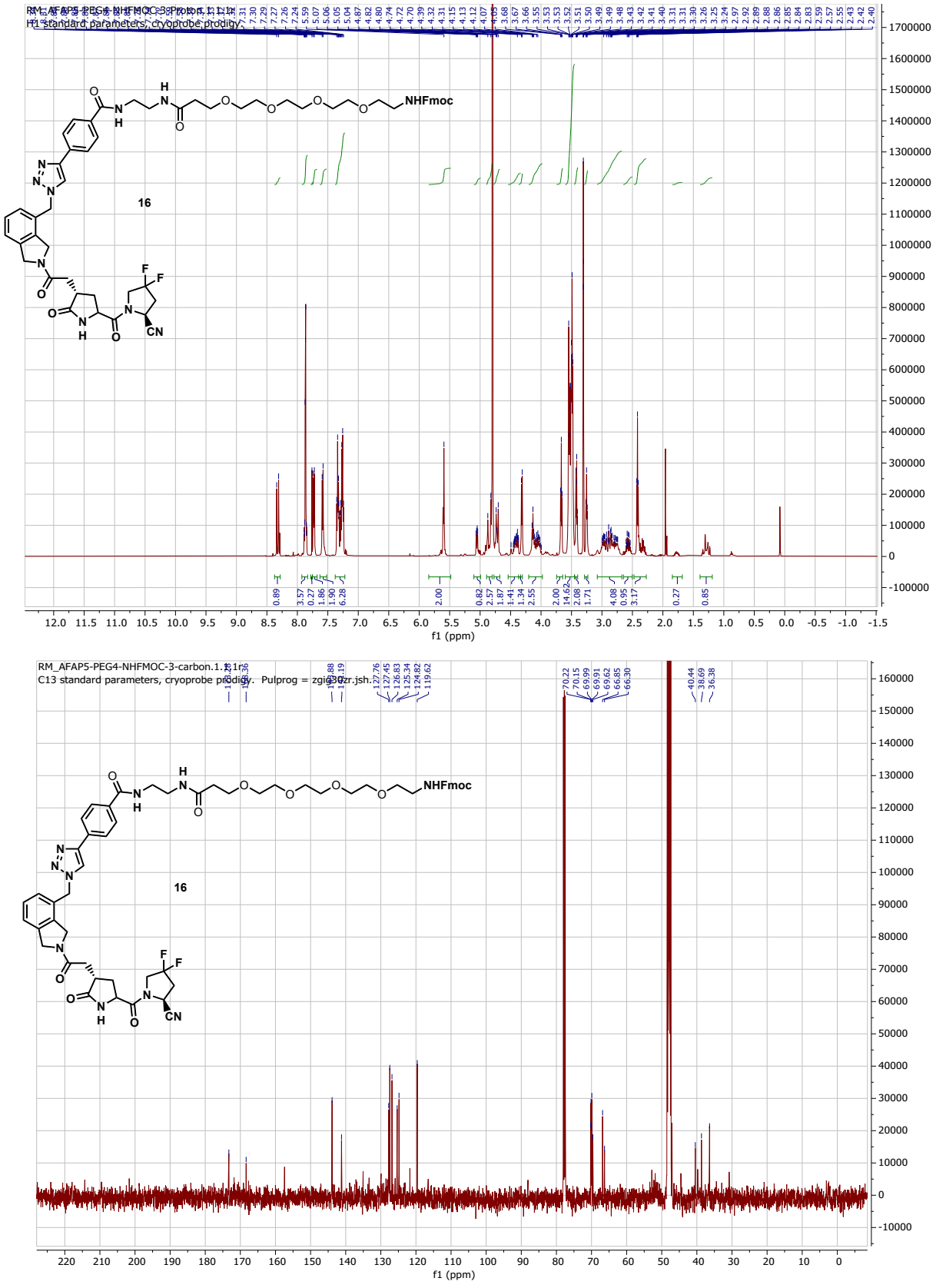

Fig. S20: ^{1}H &^{13}C NMR spectra of compound **16**

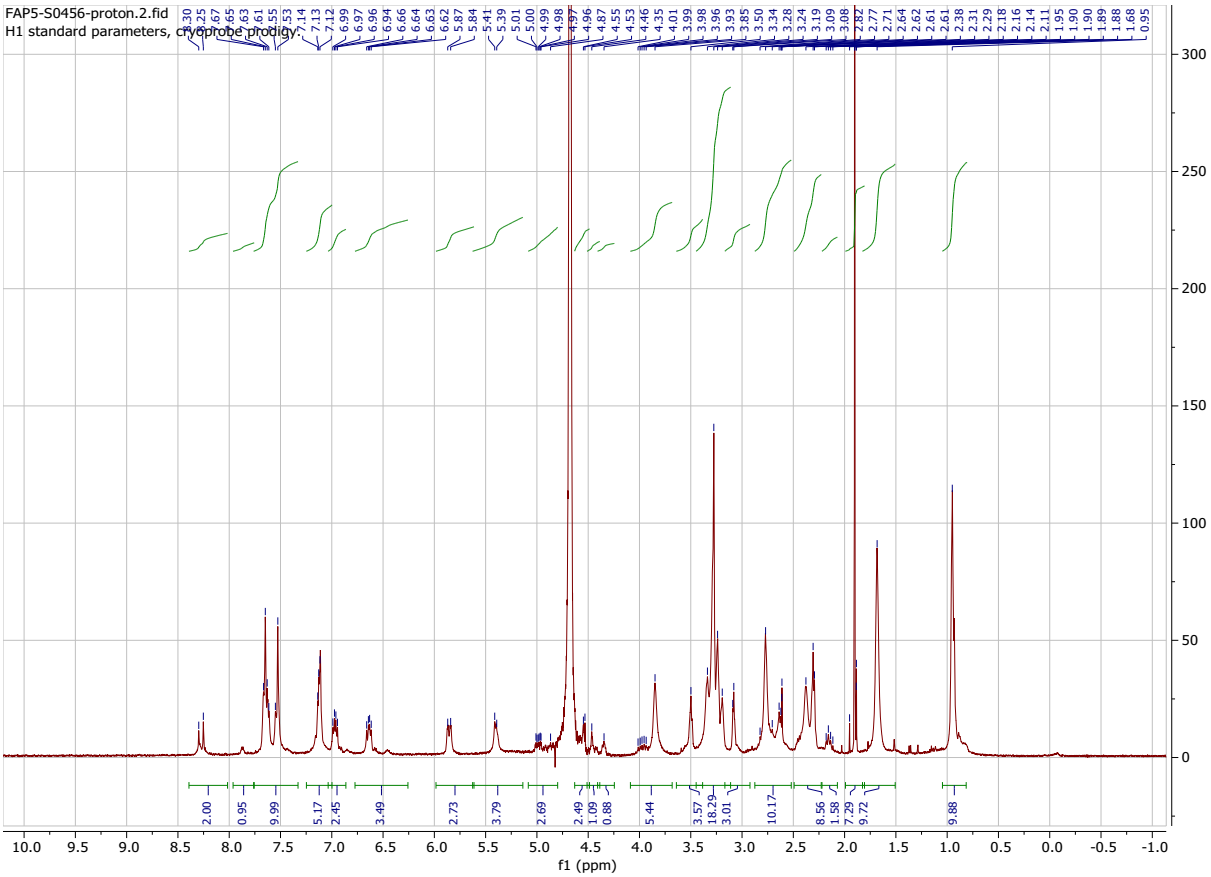

Fig. S 21: ^{1}H-NMR (D_2O) for FTL-S-S0456 (4):

Fig. S22: LC-SM of compound 14

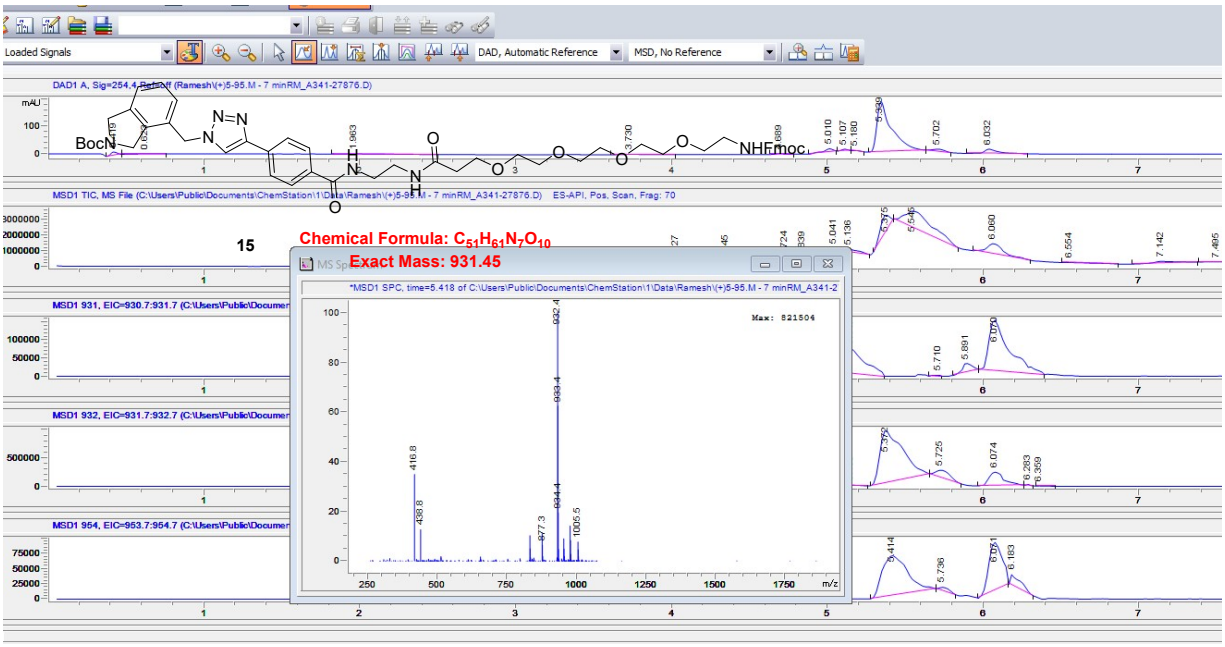

Fig. S23: LC-MS of compound 15

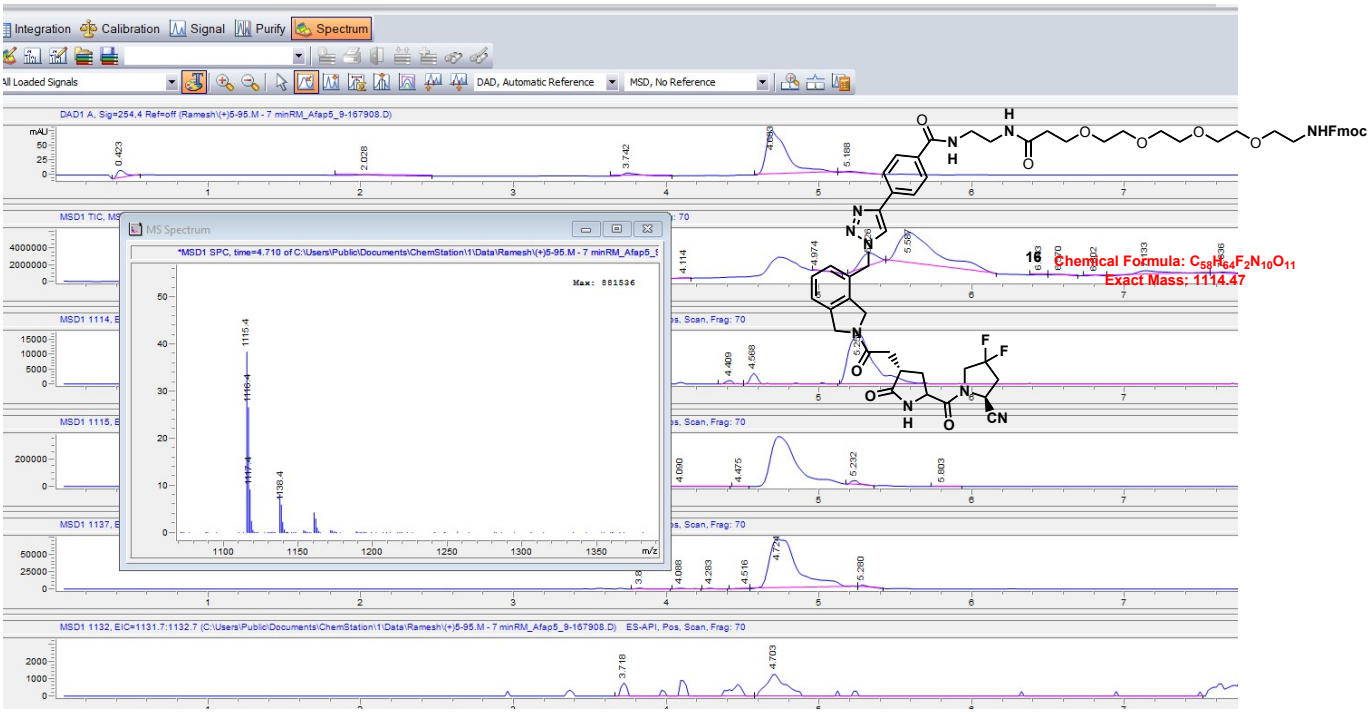

Fig. S24: LC-MS Spectra for compound 16

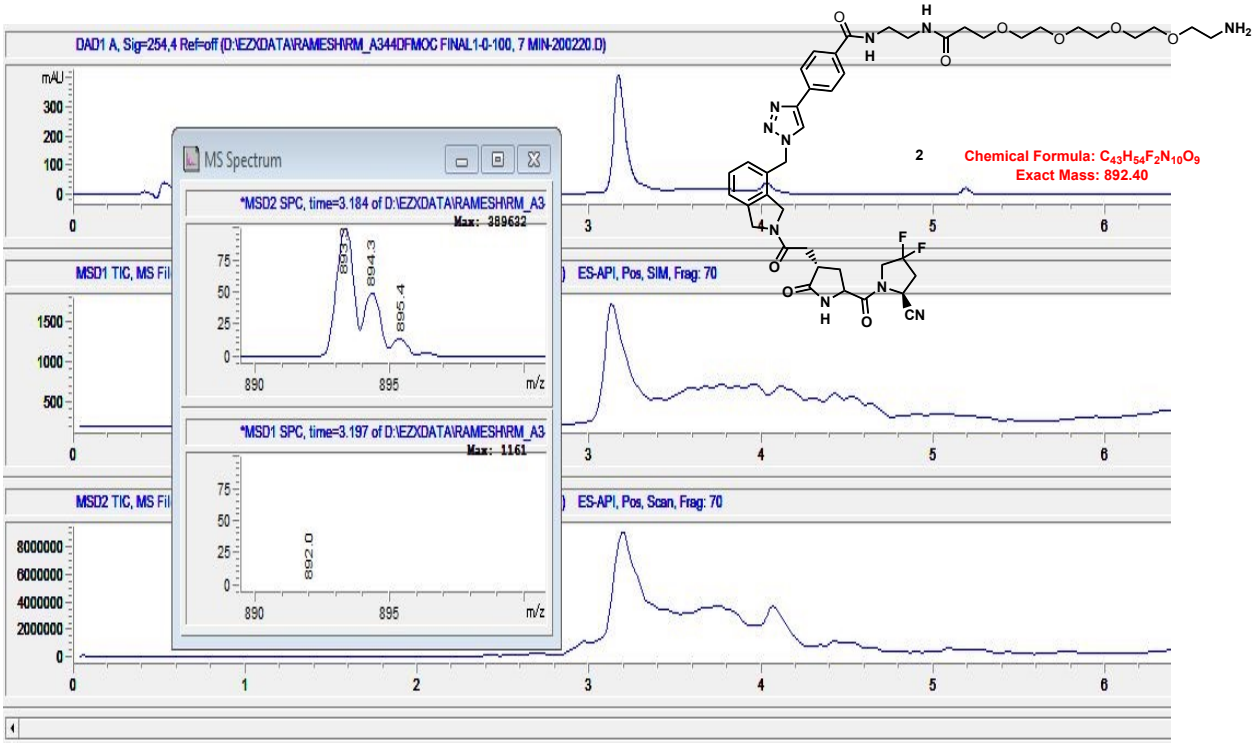

Fig. S25: LC-MS Spectra for compound 2

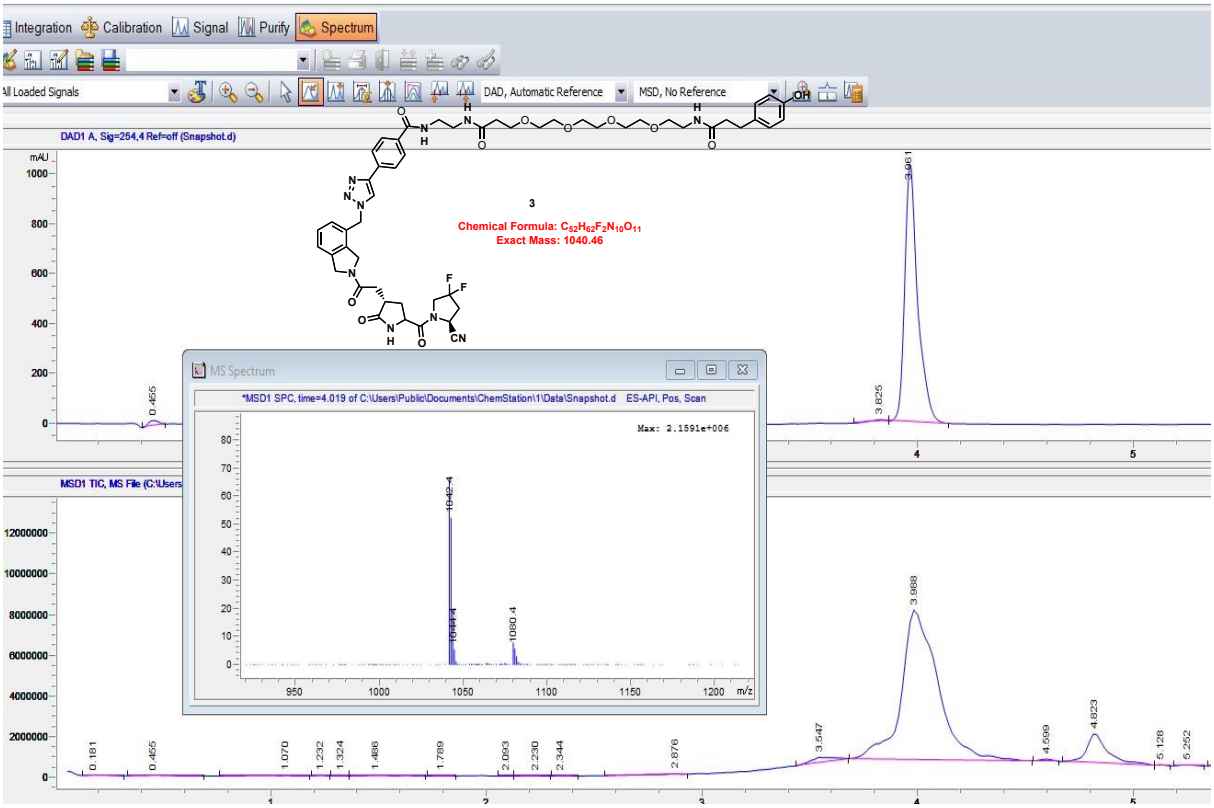

Fig. S26: LC-MS for compound 3

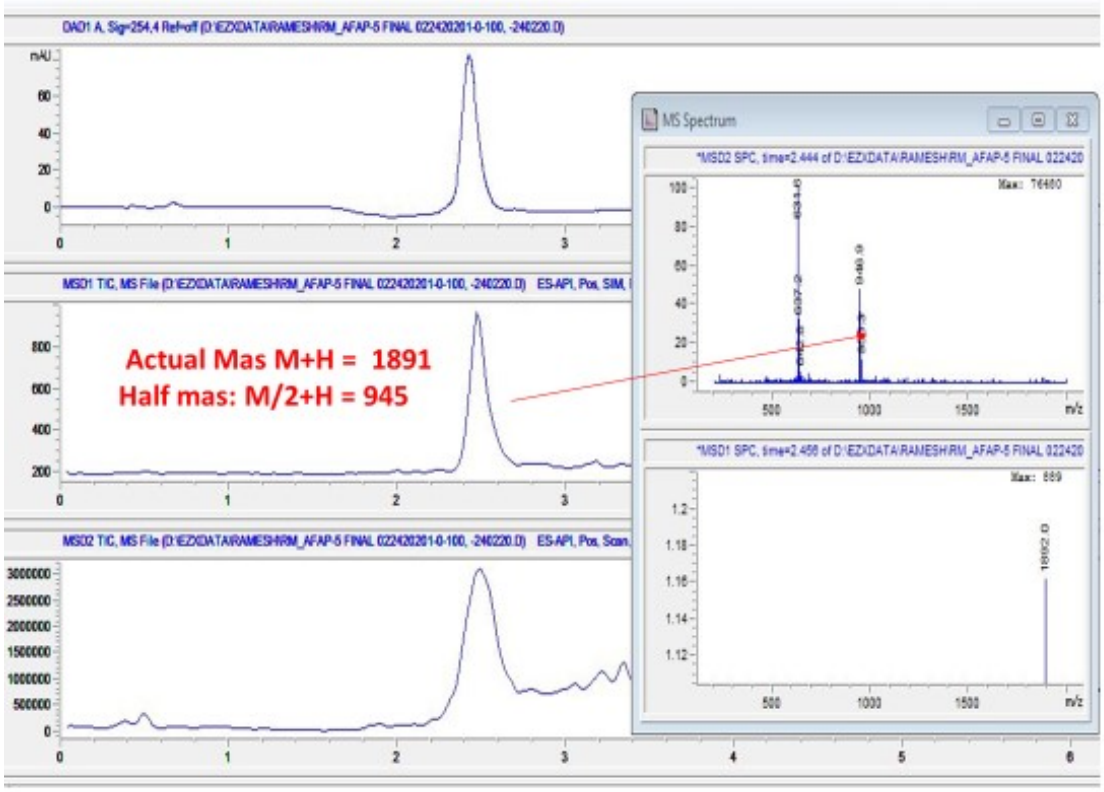

Figure 27. LC-MS of FTL-S-S0456 conjugates (4)

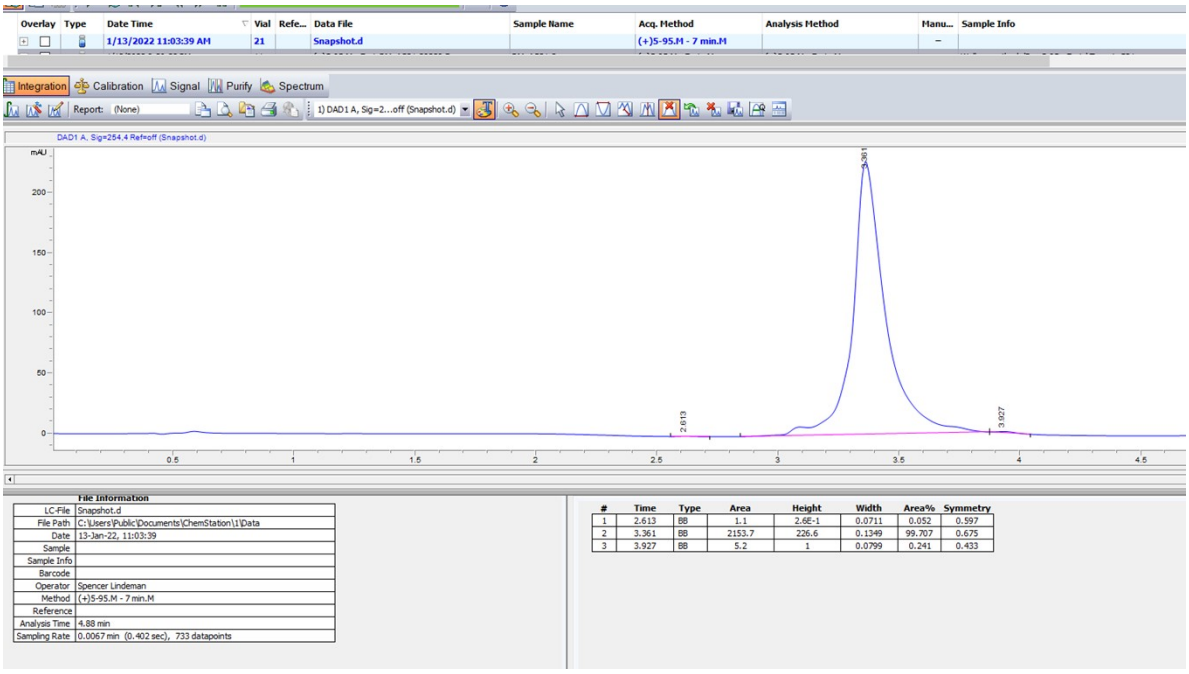

Figure 28. UV absorption peak of FTL-S-S0456 conjugate (4) in LC-MS with area under the curve analysis.

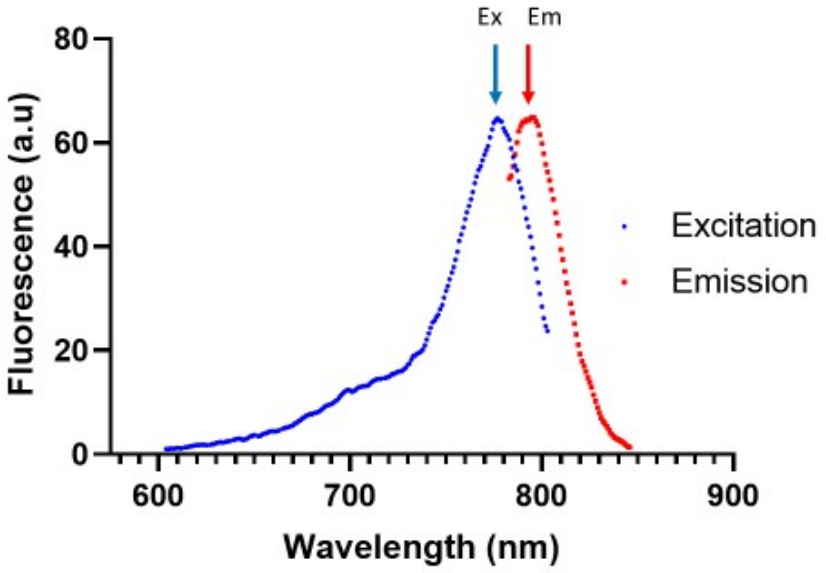

Figure 29. Excitation and emission spectra of a 1 µM solution of of FTL-S-S0456 (**4)** in PBS, pH 7.4 using λex = 776 nm and λem = 796 nm.

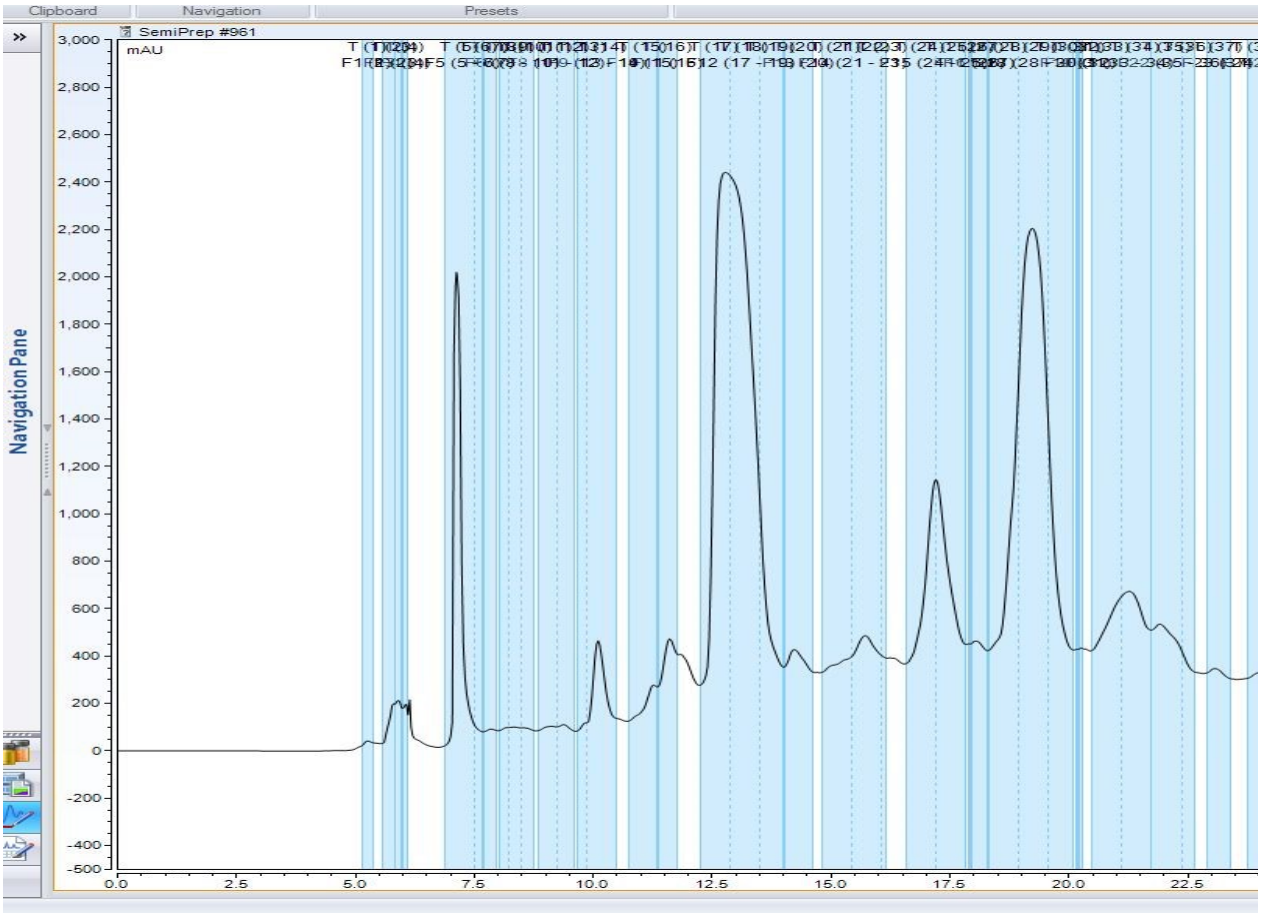

Figure S30: UHPLC Chromatogram of FTL-S -S0456 conjugate (4)

References:

1. T.-Y. Tsai, T.-K. Yeh, X. Chen, T. Hsu, Y.-C. Jao, C.-H. Huang, J.-S. Song, Y.-C. Huang, C.-H. Chien and J.-H. Chiu, *J. Med. Chem.*, 2010, **53**, 6572-6583.